Engineering Structures 167 (2018) 608–628

Contents lists available at ScienceDirect

Engineering Structures

journal homepage: www.elsevier.com/locate/engstruct

Exploring the application domain of adaptive structures

Gennaro Senatore[a,*], Philippe Duffour[b], Pete Winslow[c]

[a] Swiss Federal Institute of Technology (EPFL), School of Architecture, Civil and Environmental Engineering (ENAC), Applied Computing and Mechanics Laboratory (IMAC), Station 18, CH-1015 Lausanne, Switzerland
[b] University College London, Gower Street, WC1E 6BT London, United Kingdom
[c] Expedition Engineering, 4 Maguire St, SE1 2NQ London, United Kingdom

ARTICLE INFO

Keywords:
Adaptive structures
Active structural control
Shape control
Load-path optimisation
Whole-life energy minimisation
Structural optimisation

ABSTRACT

Using a previously developed design methodology it was shown that optimal material distribution in combination with strategic integration of the actuation system lead to significant whole-life energy savings when the design is governed by rare but strong loading events. The whole-life energy of the structure is made of an embodied part in the material and an operational part for structural adaptation. Instead of using more material to cope with the effect of loads, the actuation system redirects the internal load-path to homogenise the stresses and change the shape of the structure to keep deflections within limits.

This paper presents a systematic exploration of the domain in which adaptive two-dimensional pin-jointed structures are beneficial in terms of whole-life energy and monetary costs savings. Two case studies are considered: a vertical cantilever truss representative of a multi-storey building supported by an exoskeleton structure and a simply supported truss beam which is part of a roof system. This exploration takes five directions studying the influence of: (1) the structural topology (2) the characteristics of the load probability distribution (3) the ratio of live load over dead load (4) the aspect ratio of the structure (e.g. height-to-depth) (5) the material energy intensity factor. Results from the main five strands are combined with those from the monetary cost analysis to identify an optimal region where adaptive structures are most effective in terms of both energy and monetary savings. It was found that the optimal region is broadly that of stiffness-governed structures. For the cantilever case, the optimal region covers most of the application domain and it is not very sensitive to either live-to-dead-load or height-to-depth ratios thus showing a wide range of applicability, including ordinary loading scenarios and relatively deep structures.

1. Introduction

Adaptive structures are defined here as structures capable of counteracting actively the effect of external loads via controlled shape changes and redirection of the internal load path. These structures are integrated with sensors (e.g. strain, vision), control intelligence and actuators.

In civil engineering, active control has focussed mostly on the control of vibrations for building or bridges to improve safety and serviceability during exceptionally high loads (i.e. strong winds, earthquakes) [1,2]. Active brace systems have been tested using hydraulic actuators fitted as cross-bracing elements of the structure, controlling directly its response using actively controlled forces [3–5]. Cable stayed bridges have been controlled using the stay cables as active tendons to reduce displacements [6,7]. Active cable-tendons have also been used to change the amount of pre-stress in reinforced concrete beams and in steel trusses to limit displacements under loading [8]. The integration of actuators has been shown to be an effective way to suppress vibrations in high stiffness/weight ratio truss structures [9].

Actuation has been used to modify the membrane stress state in shell structures which are usually designed via shape optimisation methods achieving ideal geometry under permanent load. To deal with rarely occurring loading conditions different to the permanent load, additional material is distributed locally which is, therefore, only utilised during peak demands. In addition, in the event of cuttings or residual stress formed after formworks removal [10], the load carrying capacity is reduced significantly. In the event of such disturbances, actuation in the form of induced strain distributions or induced support displacements (actively controlled bearings) has been used to homogenise the stress field and in so doing minimising the maximum stress governing the design [11,12].

Active structural control has also been used in applications for shape control. Some all-weather stadia use deployable systems [13] for expandable/retractable roofs e.g. the Singapore National Stadium [14].

* Corresponding author.
E-mail address: gennaro.senatore@epfl.ch (G. Senatore).

https://doi.org/10.1016/j.engstruct.2018.03.057
Received 28 February 2017; Received in revised form 12 March 2018; Accepted 19 March 2018

Tensegrity structures consist of a set of compression and tension members whose stability relies on self-stress [15–17]. Tensegrity structures have been used for deployable systems in aerospace applications [18] and they have been investigated for force/displacement control [19–21] and frequency tuning [22] in civil engineering. Compliant structures can be thought of as structures which act like monolithic mechanisms. Compliance can be discrete or continuous. In the former, motion is allowed using flexural hinges (i.e. hinges that allows motion by bending) [23] while in the latter it is achieved through the flexibility of the constituent elements of the structure [24]. Active compliant structures have been used for the deployment of antenna reflectors [25], for the control of aircraft wings to improve on manoeuvrability [26] as well as for the control of direct daylight in buildings [27].

Adaptive structures have a good potential for mitigating strong hazard events and control of displacements and vibrations in deflection-sensitive structures [28]. Because of uncertainties regarding the long-term reliability of sensor and actuator technologies combined with long service lives of buildings and long return periods of loads, the recent trend has been to develop active structural control to help satisfying serviceability requirements rather than contributing to strength and safety improvement [29].

The potential of using adaptation to save material has been investigated by some [30–33] but whether the energy saved by using less material makes up the energy consumed through control and actuation is a question that has so far received little attention. A novel design methodology for adaptive structures was presented in Senatore et al. [34]. This method is based on improving structural performance through the reduction in the energy embodied in the material at the cost of a small increase in operational energy necessary for structural adaptation and sensing. In [35] it was shown that adaptive structures designed with this method can achieve up to 70% energy savings when compared to identical passive structures designed using state art optimisation methods. The examples studied so far range from planar portal frames and catenary arch bridges to spatial configurations of complex layout including doubly curved grid-shells and exoskeleton structures. A large scale prototype designed using this methodology was successfully tested validating key assumptions and numerical predictions [36].

These conclusions are based on a set of assumptions including the structural layout, the live load probability distribution and the material energy intensity. The purpose of this paper is to investigate how energy and monetary costs vary are as these inputs are changed via a parametric study.

2. Background: adaptive structures design methodology

In conventional design situations, members are capacity designed and the highest demand is dictated by a worst load case. However, generally building structures experience loading significantly lower than the design load, meaning that they are effectively overdesigned for most of their working life.

If the structure relies on an active system for deflection control, its stiffness can be distributed strategically such that the passive-active configuration achieves higher efficiency in terms of whole-life energy. The whole-life energy (also referred as total energy) is here understood as the sum of the embodied energy in the material and the operational energy used by the active control system. Senatore et al. [34] proposed a new design method whereby the active system is only used when necessary to ensure that the whole-life energy of the structure is kept to a minimum. The method is briefly summarised here, the reader is referred to [37] for a detailed presentation. The method has so far been implemented for reticular structures and this paper only deals with such structures. The process comprises two nested optimisation stages as shown by the flowchart in Fig. 1.

The outer optimisation stage identifies a structure with minimal overall energy (embodied + operational) for a given load probability distribution. This is done by varying the Material Utilisation Factor (MUT) which can be thought of as a scaling factor on the cross-sections. Varying the MUT changes the design from a least-weight structure with small embodied but large operational energy, to a stiffer structure with large embodied and smaller operational energy. This is shown diagrammatically in Fig. 2 which describes the notional variation of the total energy with the MUT.

The inner optimisation itself consists of two main steps. The first step finds the optimum load path and corresponding material distribution ignoring geometric compatibility and serviceability limit states thus yielding a design that represents a lower bound in terms of material mass. The optimisation is subject to equilibrium and ultimate limit state constraints including member buckling. The members of the structure are sized so that they have the capacity to meet the worst expected 'demand' from all load cases for strength only. Under external loads however, the compatible forces are in general different from the optimal forces and the resulting displacements might be beyond serviceability limits. For this reason, the second step finds the optimal actuator layout to manipulate the internal forces by changing the shape of the structure. The actuators are devices which can either reduce or increase their length and are integrated in the structure by replacing part of their elements. Via controlled actuator length changes, geometric compatibility is satisfied and at the same time deflections are controlled. For indeterminate structures, it is possible to control both the internal load-path and shape. Instead, if the structure is determinate, the active system can only control the shape because there is no self-stress state.

Once the actuator layout is known, a control strategy is determined. If a change in the loads causes a state of stress that violates a serviceability limits state (SLS), the load path is redirected and displacements are controlled by the active system. In case of a power outage or actuation system failure and concurrent occurrence of a strong event, the structure might not be serviceable but load carrying capacity is not compromised (i.e. fail-safe). In other words, the structure is designed not to collapse under the worst load case even without the contribution of the active system.

The structure is designed to take permanent loads as well as randomly fluctuating live loads. The methodology is based on the probability of occurrence of the live loads. In a real design situation, this probability should be based on empirical data or commonly used statistical models for the load considered. For illustrative purposes an example of one such probability distribution function is shown in Fig. 3(a) and (b). The method identifies the load activation threshold (the dashed line in Fig. 3a) above which actuation is needed for compensation of internal forces and displacements. Fig. 3(b) plots the hours of occurrence for each level of the load obtained by discretising the probability density distribution scaled by the total number of hours of service. The introduction of the load activation threshold shows how passive and active design can be combined to reach a higher level of efficiency.

3. Parametric exploration

3.1. Scope

The parametric study carried out in this paper has five main objectives:

1. Compare statically indeterminate against determinate structures to appreciate the influence of the load-path redirection on operational energy consumption;
2. Appreciate the sensitivity of the energy savings to features of the probability of occurrence of external loads;
3. Appreciate the sensitivity of the energy savings to the live load to dead load (L/D) ratio;
4. Study the importance of the slenderness of the structure by varying

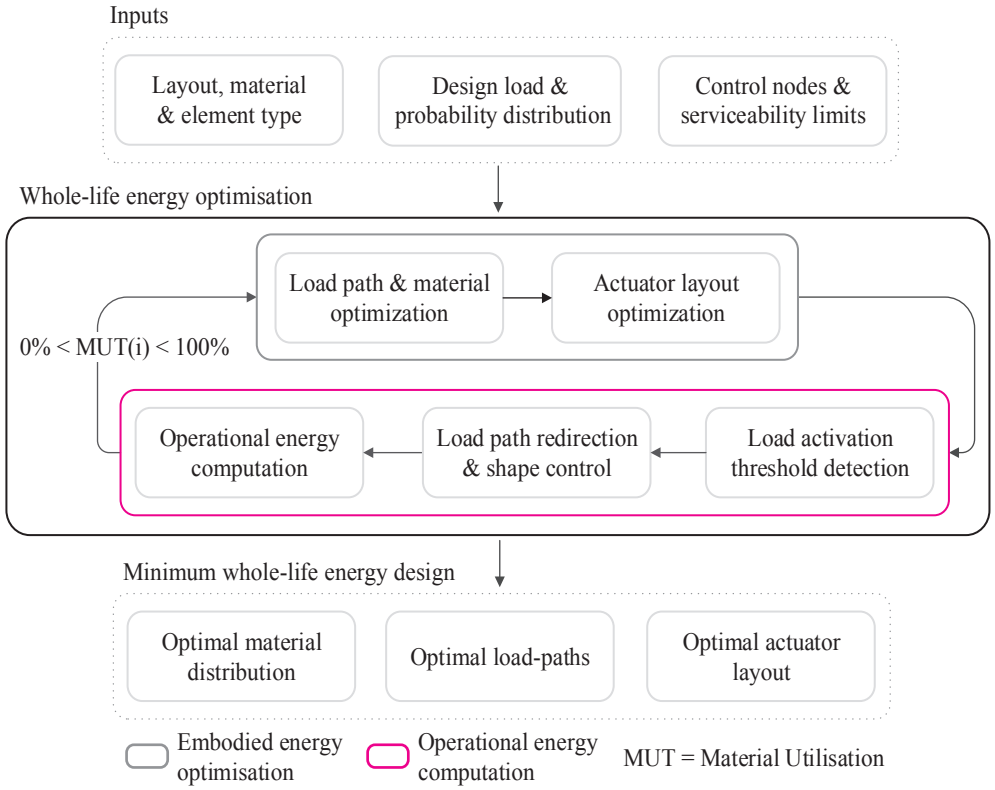

Fig. 1. Design methodology flowchart. @IOP Publishing. Reproduced with permission. All rights reserved [36].

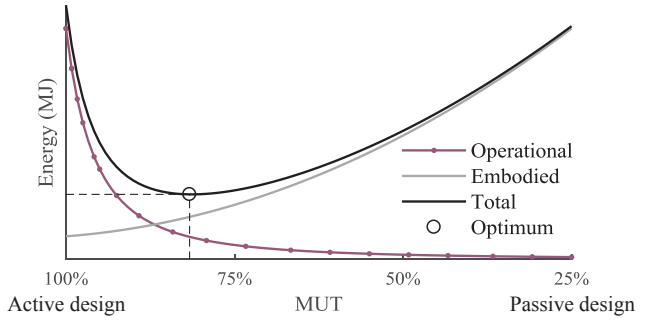

Fig. 2. Embodied, operational and whole-life energy as a function of the material utilisation factor (MUT). @IOP Publishing. Reproduced with permission. All rights reserved [36].

main geometrical features such as height-to-depth (H/D) or span-to-depth (S/D) ratio;

5. Appreciate the importance of the embodied energy compared to the operational energy by varying the material energy intensity (MEI) factor.

In addition, a monetary cost analysis is carried out to investigate whether the energy savings translate into monetary cost savings. The results from the main strands will be combined with those from the monetary cost analysis to identify an optimal region where adaptive structures are most effective in terms of both energy and monetary cost.

3.2. General assumptions

3.2.1. Actuator type, dynamics and control system energy consumption

It is assumed that linear actuators are used with a mechanical efficiency of 80%. For civil engineering structures, the force magnitudes to be controlled will likely orient the choice to hydraulic actuators. The mechanical efficiency of hydraulic actuators is in a range of 90–98% [38]. For this reason, the assumption on the mechanical efficiency of the actuators is conservatives.

The frequency response of the actuators is set to the 1st natural frequency of the structure as this is likely to be the frequency that will dominate the response of most lightly damped structures excited by wind, earthquakes or pedestrians. This assumption is conservative because it implies that even for quasi-static or low frequency response, the actuators will always work at the 1st natural frequency of the structure.

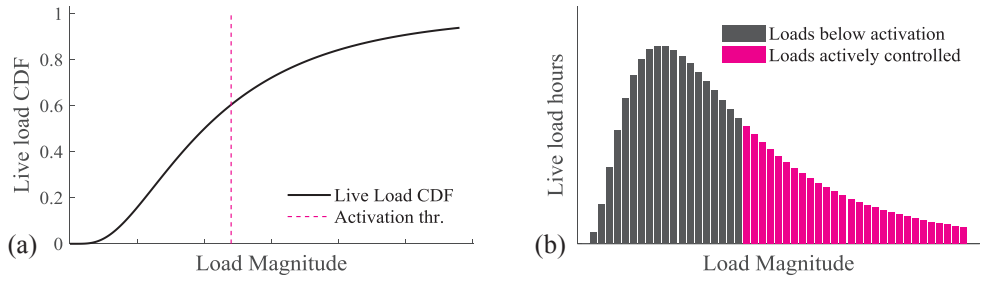

Fig. 3. (a) Live load cumulative distribution; (b) live load hours. @IOP Publishing. Reproduced with permission. All rights reserved [36].

I assumed that non-active means are used to control vibrations (e.g. tuned mass dampers) if required. This is the case when vibrations are caused by loads below the activation threshold (ULS and SLS respected). Whilst the active system could be used to compensate this effect, it may come at the expense of a significant additional operational energy since vibrations can occur very often.

The energy it takes to power the control system (e.g. sensors and signal processing) is modelled here as a linear function of the number of structural elements and actuators. This assumption is based on empirical knowledge gained via experimental testing on a large scale adaptive truss prototype [36]. Note that the control system energy is part of the total operational energy but it is not related to the energy needed for structural adaptation (i.e. for force and shape control). The former is usually substantially lower than the latter. The control system energy requirement becomes important for small structures because in this case it is comparable with the embodied energy savings.

3.2.2. Control system integration

It is assumed that the structures are fitted with as many strain sensors as necessary to be able to compute the displacement field with sufficient accuracy.

The actuators are thought of as integrated into the structure by replacing part of its elements. As shown in Senatore et al. [37], the actuators positions can be determined selecting those elements whose length changes contribute most efficiently to correct the internal forces and displacements. This analysis requires as input the selection of a certain number of degrees of freedom to be controlled. The choice of the controlled degrees of freedom is up to the designer and is usually dictated by serviceability. The minimum number of actuators n^{ACTs} to control exactly the desired displacements is equal to the number of controlled degrees of freedom n^{CDOFs} plus the degree of indeterminacy of the structure ($n^{ACTs} = n^{CDOFs} + r$). This is the minimum number of actuators needed to turn the structure into a controlled mechanism. If fewer actuators are utilised, displacements can be controlled approximately.

3.2.3. Statistical modelling of the load

The structures are designed to take a generic permanent load (e.g. self-weight + cladding) as well as a randomly fluctuating one such as wind, earthquakes, crowd loading or moving loads such as trains. For simplicity, these loads are all considered as live loads. The statistics of this live load are modelled using a log-normal probability distribution (Fig. 3) because this distribution is closely related to the normal distribution, hence it is general only taking positive real values and thus it provides the desired bias toward the lower values of the random variable.

The live load magnitudes used in this paper are commensurate with the loads used by practicing design engineers. The design load (excluding safety factor), thereafter called the characteristic load is normally set to the 95th percentile of the load probability distribution. However, other characteristic loads (e.g. 99th or 85th percentile) will be considered in Section 5. The probability distribution only describes the occurrence of the live load. For simplicity, the mean of the underlying normal distribution is set to zero. Once the mean and the characteristic load are set, the standard deviation can be determined. For all case studies discussed in this paper the structure service life is set to 50 years.

3.3. Comparison adaptive vs passive

The metrics considered for the adaptive vs passive comparison are mass and total energy savings. The passive structure is designed using an optimisation routine described in Senatore [39] that outperforms the Modified Fully Utilised Design Method (Patnaik et al. [40]). The energy savings are defined as the difference between the embodied energy of the passive structure and the total energy of the adaptive one divided by the former.

3.3.1. Structural elements and material energy intensity (MJ)

All structural elements have a cylindrical hollow section. To limit the optimisation process complexity, the wall thickness is set to 5% of the external diameter. The mass of an actuator is assumed to be a linear function of the required force with a constant 0.1 kg/kN (e.g. an actuator with a push/pull load of 1000 tons weighs 1000 kg) [41].

The energy analysis is carried out using a material energy intensity factor (MEI) to convert the material mass into embodied energy. The material utilised in the simulations described in this paper is steel in the form of rods obtained from predominantly virgin materials (no recycled content) whose energy intensity is 35 MJ/kg [42].

3.3.2. Ultimate and serviceability limit state

Both passive and adaptive structures are subject to the same load factors and ultimate limit state constraints including member buckling. The limits on deflection used in the examples described in this paper are those commonly used for the design of civil engineering structures. To make a fair comparison between adaptive and passive structures, the displacements are assumed to be caused by the live load only. The passive structure is thought of as perfectly pre-cambered under the permanent load. Hence the material distribution is driven to compensate for deflections caused by the live load only. For the adaptive structure, instead, the actuators reduce completely the displacements caused by the permanent load. In this way, both the passive and the adaptive structures will already be stressed when the live load is applied.

3.4. Case studies

Throughout this parametric exploration, the structural configurations under consideration will be a vertical cantilever and a horizontal simply supported truss.

For the cantilever case, each truss can be thought of as the exoskeleton of a multi-storey building shown in Fig. 4(a). Several heights (H) and height-to-depth (H/D) ratios will be tested. The floor perimeter of the building is kept square. For simplicity, due to symmetry the design of the structure is reduced to that of one planar truss. Fig. 4(b) shows the statically indeterminate sample with a H/D ratio of 10. Fig. 4(c) shows the corresponding statically determinate topology.

The horizontal displacements of all the unconstrained nodes are set as controlled degrees of freedom (CDOFs) which are indicated by circles in Fig. 4(b) and (c). The total building drift is limited to height/500 [43].

There are three load cases, L1 is self-weight + dead load; L2 and L3 represent wind loads (live loads) acting in opposite directions. Their intensity varies parabolically with height. The dead load is distributed on the floor area $A^{Dead} = D \cdot D$ and it is applied every 4 m along the height of the structure. The wind loads are applied on the façade area $A^{Live} = H \cdot D$ on both sides using a pressure coefficient of 0.5 for the downwind side [44]. Table 1 gives the three load combinations considered for this case study.

For the simply supported case, each truss is part of roof supporting system shown in Fig. 5(a). Several spans (S) and span-to-depth (S/D) ratios will be tested. Fig. 5(b) shows a statically indeterminate sample with an (S/D) of 20 and (c) show the corresponding statically determinate topology. The vertical displacements of all the nodes except

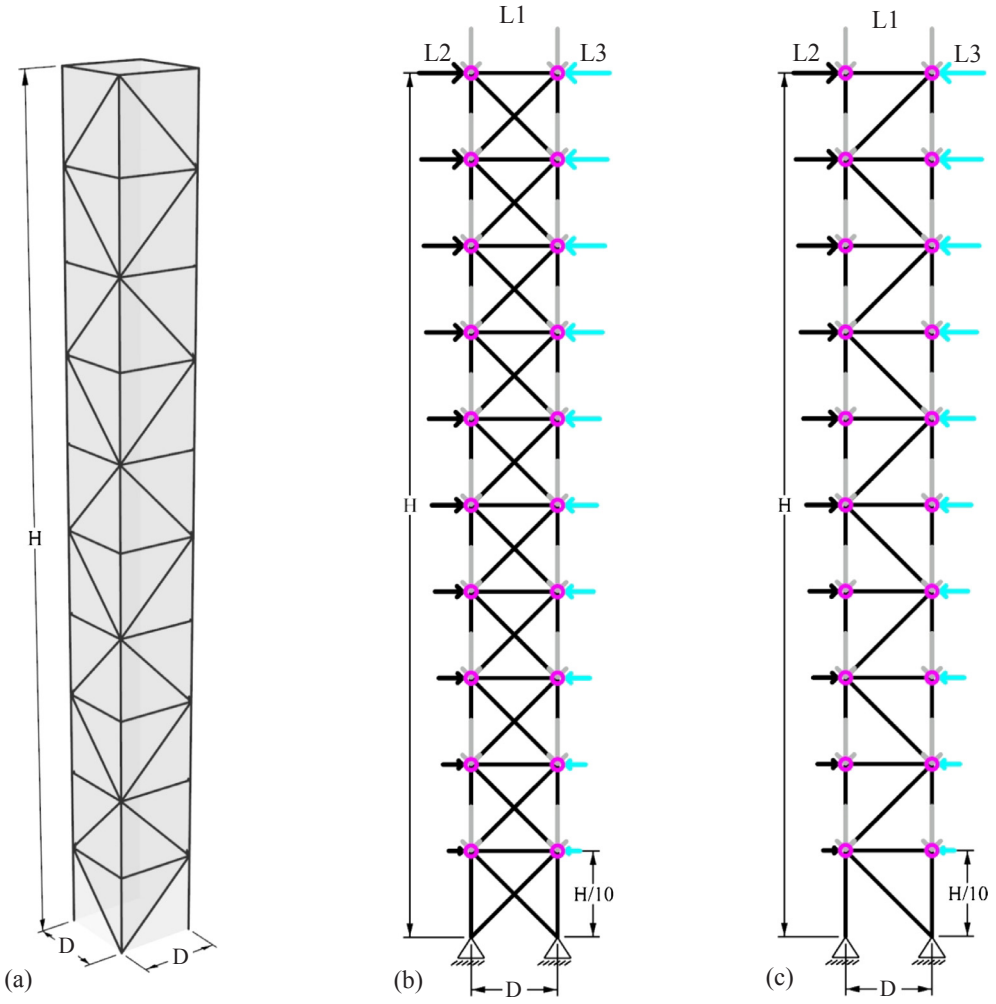

Fig. 4. (a) Exoskeleton structure; (b) indeterminate, (c) determinate; controlled nodes indicated by circles.

Table 1
Cantilever|load combination cases.

Case	Load factor	Permanent load	Load factor	Live load
LC1	1.35	L1 = dead load + self	1.5	n/a
LC2	1.35	L1 = dead load + self	1.5	L2
LC3	1.35	L1 = dead load + self	1.5	L3

the supports of the top chord are set as controlled degrees of freedom which are indicated by circles in Fig. 5. Deflections are limited to span/360.

There are two load cases, L1 is self-weight + dead load; L2 is an upward load which is representative of the suction caused by a wind type load. Each bay of the truss supports a subsidiary area $A = S{\cdot}S^{Op}$ out of plane as shown in Fig. 5(a) where S^{Op} is the length of the out of plane span. Table 2 gives the two load combinations aconsidered for this case study.

For both structural configurations, it is assumed that lateral stability in the other direction is provided by some other means. In both cases, the dead load is set to 3 kN/m^2 and the live load maximum intensity is set proportional to the dead load via the live-to-dead-load (L/D) ratio. The intensity of the live load is determined via the L/D ratio which will be varied in a range from 0.1 to 2. This gives a 0.3 kN/m^2 to 6.0 kN/m^2 live load which can be thought of as resulting from wind pressure caused by a category 1 to 3 hurricane respectively (wind velocity between 100 km/h and 200 km/h). The hurricane intensity refers to the Saffir-Simpson scale whose highest category is 5. This way, the live load relates to the dead load representing realistic loading scenarios.

In general, the geometry of the truss bay is not an important parameter as long as extreme aspect ratios are avoided. For this reason, the truss bay aspect ratio is set as a linear function of the height or the span with a proportional constant of 1/10 (H/10 in Fig. 4 and S/10 in Fig. 5). This avoids very long truss elements which would be impractical for transportation and conversely too short elements which would make fabrication extremely difficult. Note that because member instability is part of the optimization constraints, all element capacities satisfy ultimate limit states.

4. Energy savings vs topology

In this section a statically determinate truss is compared to a statically indeterminate one for both cantilever and simply supported case. The aim is to assess the effect of the structural topology and the load path redirection on material distribution and the implications on operational energy consumption.

4.1. Cantilever case|determinate vs indeterminate

The structure considered in this study is a 400 m tall cantilever truss whose H/D ratio is set to 10. Both the height and H/D ratio are mid

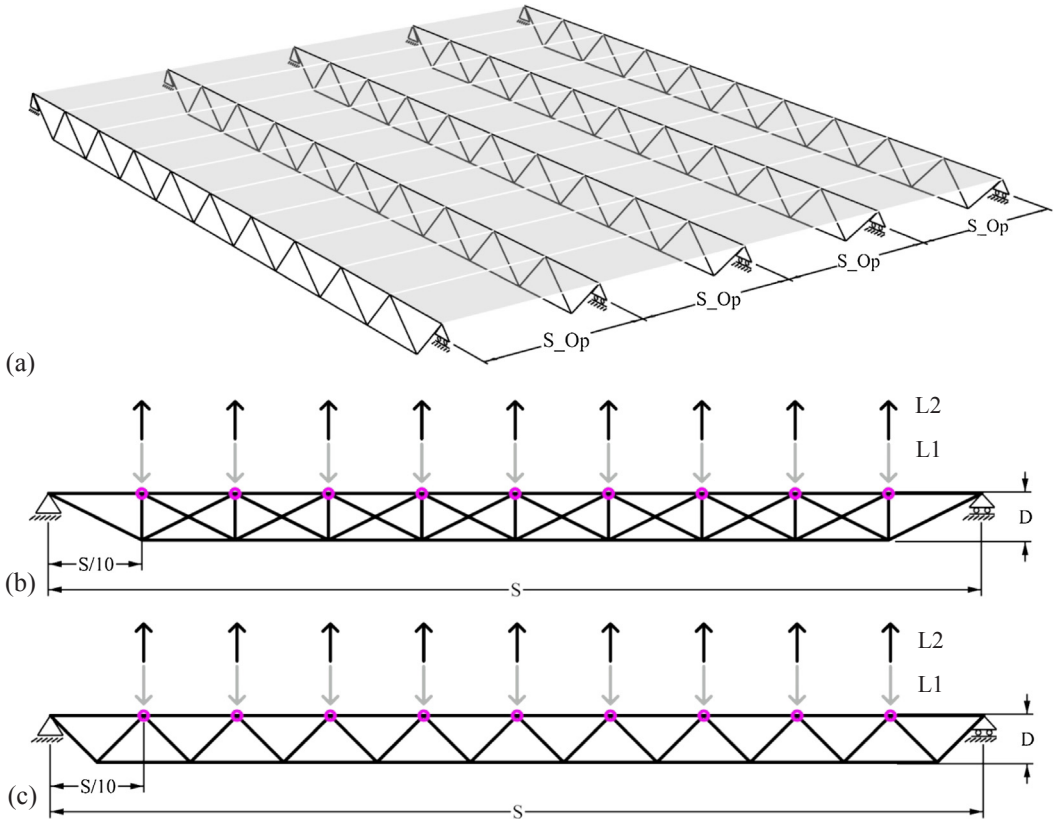

Fig. 5. (a) Roof structure; static (b) indeterminate, (c) determinate – controlled nodes indicated by circles.

Table 2
Simply supported|load combination cases.

Case	Load factor	Permanent load	Load factor	Live load
LC1	1.35	L1 = dead load + self	1.5	n/a
LC2	0.9	L1 = dead load + self	1.5	L2

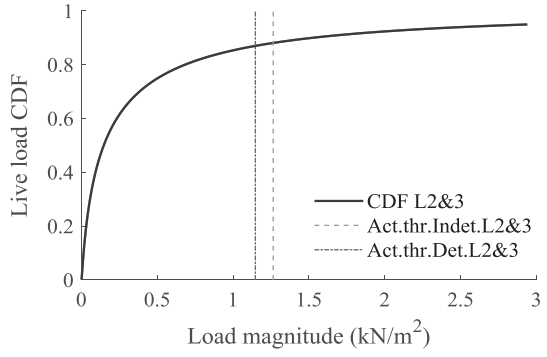

Fig. 6. Live load cumulative distribution function (CDF) and load activation threshold.

value in the range that will be investigated in Section 6. There is a total of 20 controlled degrees of freedom indicated by circles in Fig. 4. The minimum number of actuators to control exactly the controlled nodes is 20 and 30 for the statically determinate and indeterminate (indeterminacy is 10) structures respectively (Section 3.2.2). The dead load is set to 3 kN/m^2 each truss supporting 40 m of out of plane span resulting in a UDL of 120 kN/m. The live load cases described in table 1 and illustrated in Fig. 4 are applied. The L/D ratio is set to 1.

Fig. 6 shows the live load cumulative distributions functions (CDFs) for the two cases LC2 and LC3 plotted on the same chart (the loads have opposite directions but identical probability distributions). The vertical dashed line represents the activation threshold for the indeterminate case which is identical for both L2 and L3 because of symmetry. Similarly, the dash-dotted line represents the activation threshold for the determinate case which is slightly lower compared to that of the indeterminate case. Consequently, the total actuation time required to compensate for displacements is 3.6 and 4 years for the indeterminate and determinate case respectively.

Fig. 7(a) shows the embodied, operational and total energy as functions of the MUT, the dashed lines representing the indeterminate case. For the determinate case, the optimal adaptive configuration is obtained for an MUT of 68% whilst the passive structure corresponds to an MUT of 31%. This means that the adaptive and passive structures are designed so that the maximum stress under the worst load combination is 68% and 31% of the yield stress respectively. Similar considerations apply for the indeterminate case. In terms of total energy savings, the indeterminate and determinate adaptive structures achieve 33% and 36% respectively compared to the passive structures as shown by the bar chart in Fig. 7(b); mass savings are 55% and 58% respectively.

Fig. 8 compares the optimised passive structure (a) with the adaptive structure (b). The actuators are represented by bigger diameter cylinders replacing the central part of the elements they are fitted onto. Fig. 8(c) shows both the controlled shape and the deformed shape

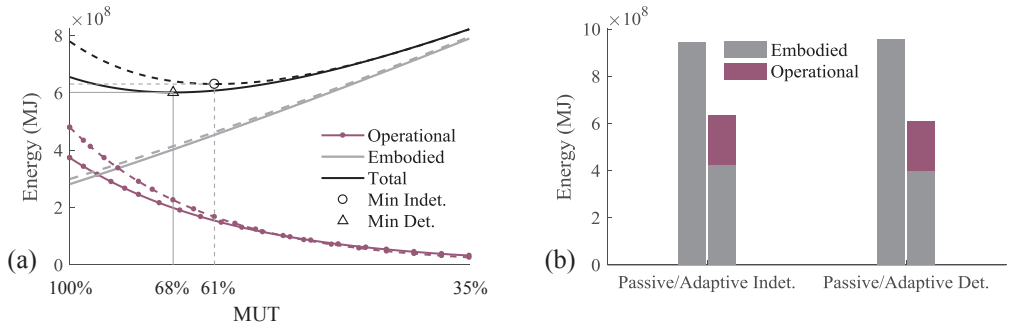

Fig. 7. Cantilever case; (a) Total energy vs material utilisation factor (MUT) for indeterminate (dashed) and determinate (solid) case; (b) passive vs adaptive total energy.

under LC2. Without active displacement compensation (i.e. shape change), the tip deflection is 1969 mm which is beyond serviceability limit (height/500 = 800 mm). Fig. 8(d) shows the optimal load path and the force redirection (e), difference between optimal and compatible load paths for LC2. Referring to Fig. 8(e), it can be appreciated the internal forces are redirected alternating tension and compression in the bracers every other bay.

Fig. 9 shows the comparison between passive (a) and adaptive (b) as well as deformed and controlled shape (c) and optimal forces (d) for the determinate case. Note that for statically determinate structures optimal and compatible forces are identical hence no load-path redirection occurs.

Comparing Fig. 8 with Fig. 9, it can be observed that material distribution as well as controlled and non-controlled displacement fields are similar between the indeterminate and determinate trusses. There are more elements (50) in the indeterminate truss with respect to the

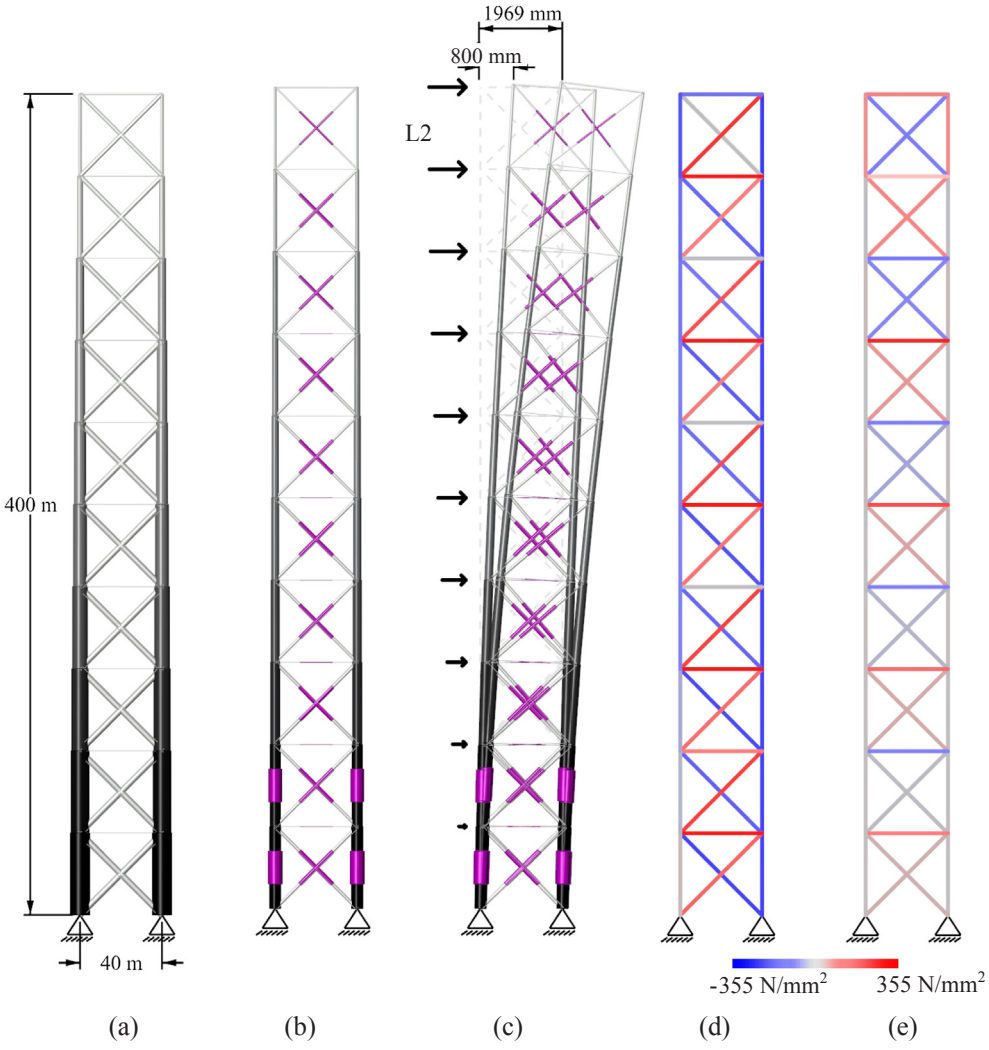

Fig. 8. Cantilever truss statically indeterminate (a) passive and (b) adaptive solution; (c) controlled and non-controlled shape under LC2, mag. ×20; (d) optimal load-path and (e) force redirection under LC2. Scale 1:4000.

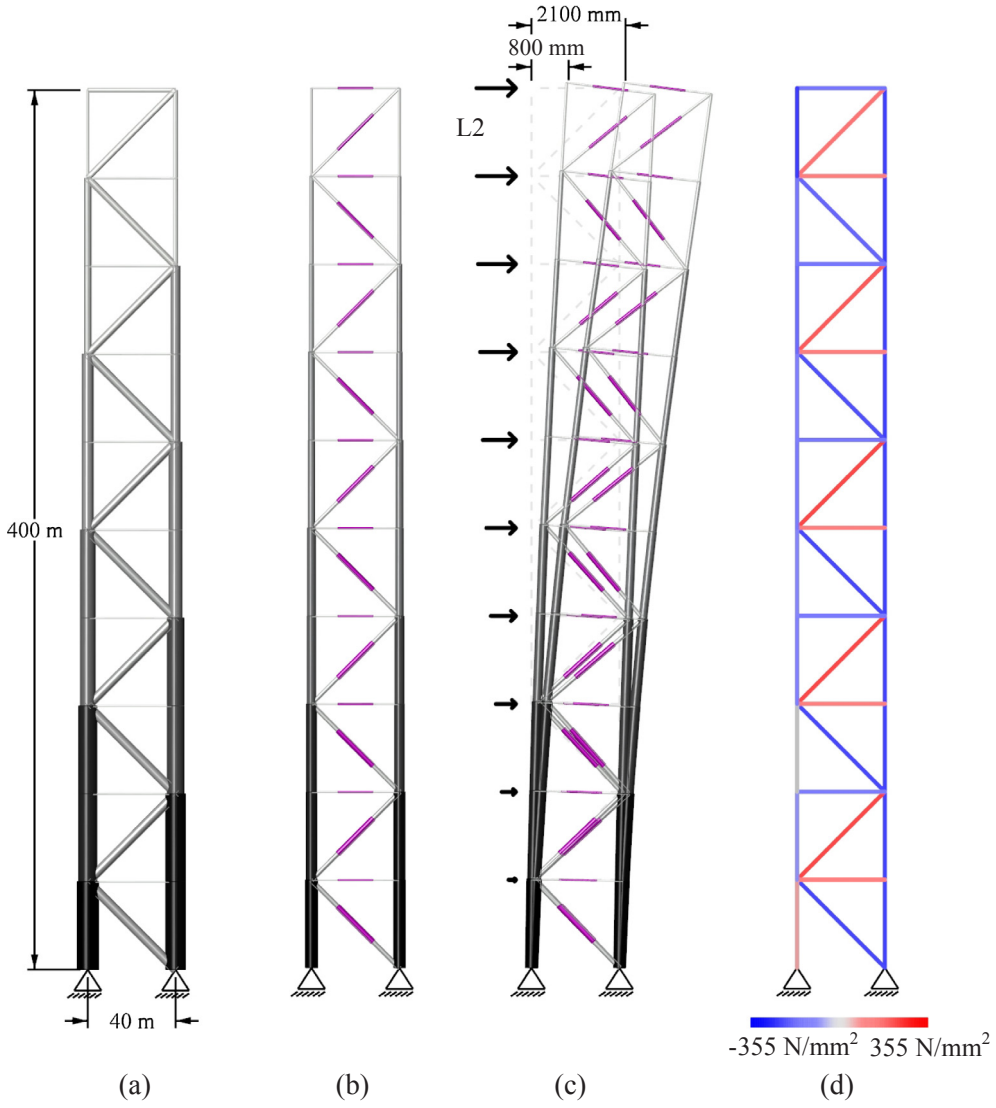

Fig. 9. Cantilever truss statically determinate (a) passive and (b) adaptive solution; (c) controlled and non-controlled shape under LC2, mag. ×20; (d) optimal load-path under LC2. Scale 1:4000.

determinate one (40) resulting into a slightly higher embodied energy for the former because the cross-section area lower bound is set identical for both cases. The load path redirection occurring in the indeterminate structure has little effect on the operational energy.

4.2. Simply supported case|determinate vs indeterminate

The structure considered in this study is a 100 m span simply supported truss with a S/D ratio set to 20. Both the span and S/D ratio are mid value of the range that will be investigated in Section 6. There is a total of 9 controlled degrees of freedom (CDOFs) indicated by circles in Fig. 5. The minimum number of actuators to control exactly the desired displacements is 9 and 17 for the determinate and indeterminate (indeterminacy of 8) case respectively (Section 3.2.2). The dead load is set to 3 kN/m^2 each truss supporting a 10 m out of plane span (S^{Op}) resulting in a UDL of 30 kN/m. The live load cases described in table 2 and illustrated in Fig. 5 are applied, the L/D ratio is set to 1.5 (live load max intensity of 4.5 kN/m^2).

Similar to the cantilever case, the indeterminate and determinate adaptive simply supported trusses have similar activation thresholds. The total time during which actuation is required to compensate for displacements is 2.5 and 2.1 years for the indeterminate and determinate structure respectively. Fig. 10(a) shows the embodied, operational and total energy functions of the MUT. Total energy savings are 25% and 30% for the indeterminate and determinate case respectively compared to their corresponding passive structures as shown by the bar chart in Fig. 10(b); mass savings are 45% and 42% respectively.

Figs. 11 and 12 compare the optimised passive structures (a) with the adaptive structures (b) showing the optimal load-paths in (c). Fig. 11(d) and (e) show the stress redirection and non-controlled stress flow respectively. Internal forces are redirected by adding compressive forces in the bracers located at mid span (Fig. 11d) which would be in tension without active control due to the upward external load (Fig. 11e). In addition, tensile forces are added to all vertical elements between top and bottom chords. Without active displacement compensation (i.e. shape change), the mid-span deflections are 492 mm and

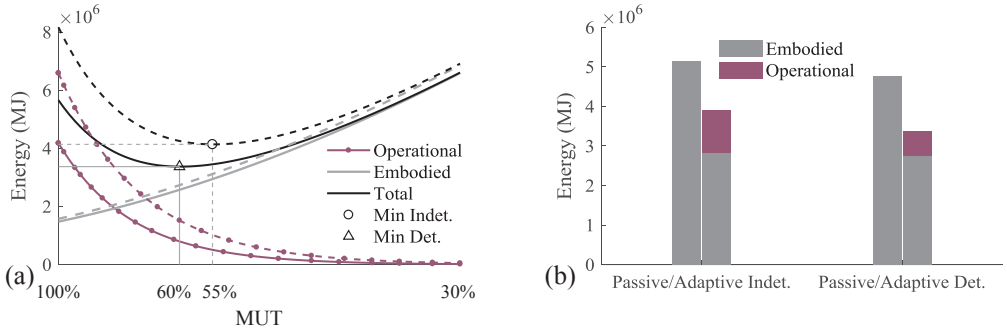

Fig. 10. Simply supported case; (a) Total energy vs material utilisation factor (MUT) for indeterminate (dashed) and determinate (solid) case; (b) energy comparison.

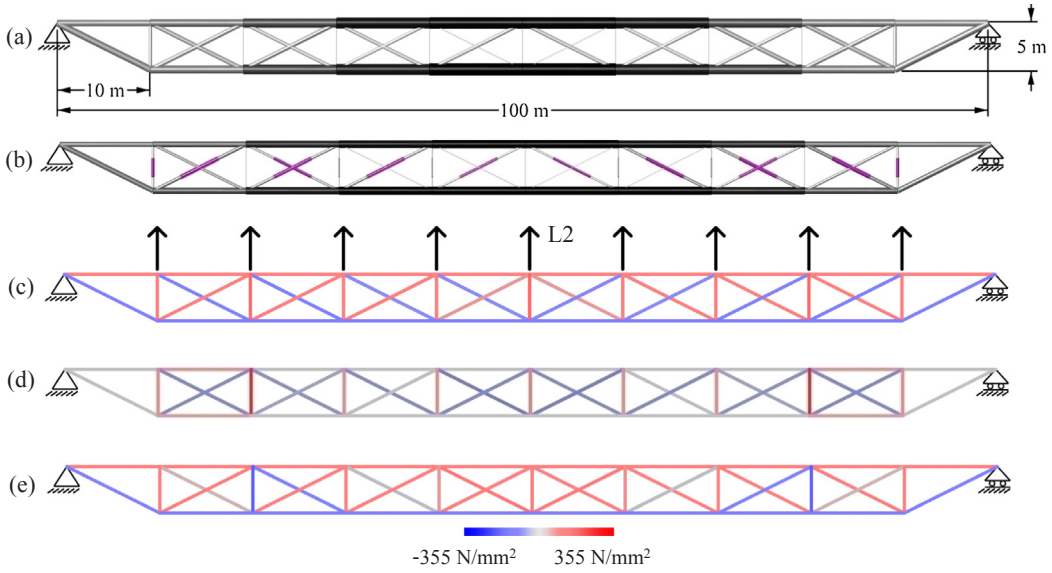

Fig. 11. Simply supported truss beam statically indeterminate (a) passive and (b) adaptive solution; (c) optimal (controlled) load-path, (d) force redirection under LC2 and (e) non-controlled forces. Scale 1:800.

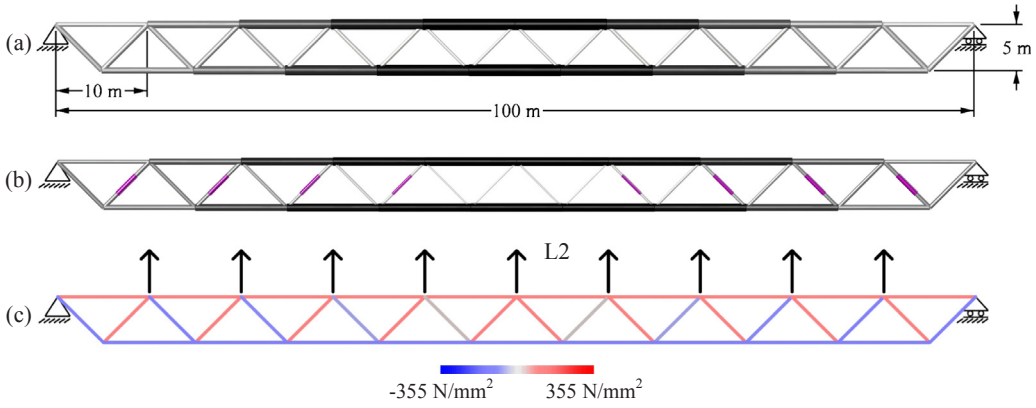

Fig. 12. Simply supported truss beam statically determinate (a) passive and (b) adaptive solution; (c) optimal load-path under LC2. Scale 1:800.

528 mm for the determinate and indeterminate case respectively which is beyond serviceability limit (span/360 = 277 mm).

As for the cantilever case, the indeterminate and determinate adaptive simply supported trusses have a similar behaviour both in terms of displacement compensation and energy savings. However, in this case the force redirection has a substantial effect on the operational energy which is almost double that of the determinate case.

4.3. Conclusions topology study

Following from the results shown in this section, it can be said that the energy performances of a planar truss will be similar whether it is statically determinate or indeterminate. Due to the similarity of the energy savings between the two cases, the remainder of this parametric exploration will be carried out on the statically determinate topology. The simplicity of the statically determinate structure will help assess

relationships between parameters of interest (Section 3.1) avoiding potential numerical issues that can arise with more complex layouts.

5. Energy savings vs characteristic loads

The characteristic load considered so far has been set to the 95th percentile of the load probability distribution (a log-normal function) for each load case (Section 3.2.3). In this section, three load probability distributions with identical mean but characteristic loads set to the 85th, 95th and 99th percentile are considered. Setting the characteristic load to the 85th percentile means that high levels of the live load are more likely to occur compared to a characteristic load set to the 95th or 99th percentile. The structures considered in this study are the same statically determinate cantilevered and simply supported trusses considered in the previous section. The L/D ratio is kept at 1 for the cantilever and 1.5 for the simply supported truss.

Fig. 13 shows the live load cumulative distribution functions and the activation threshold (indicated by dashed lines) for the cantilever (a) and simply supported case (b). As expected, it is found that the activation threshold is pushed towards higher values the higher the probability of occurrence (CL = 85%) of the live load to reduce the operational energy.

Fig. 14(a) shows the operational, embodied and total energy as functions of the MUT for the cantilever case. The curves correspond to the live load probability distributions with a characteristic load set to the 85th (dashed), 95th (solid) and 99th (dash-dot) percentile. As expected, if higher levels of the live load are more likely to occur (e.g. characteristic load set to the 85th percentile), the optimal configuration is obtaeind for a lower MUT because it is more effective to rely on passive resistance (material mass) to minimise the whole-life energy. The opposite happens when the characteristic load is set to 99th percentile. Fig. 14(b) shows the bar chart of the total energy for the passive structure and the three adaptive solutions obtained for each characteristic load. There is a 15% loss in energy savings when moving from the 99th to the 95th percentile but only 5% loss when moving from the 95th to the 85th percentile. Similar results are obtained for the simply supported case as shown by the energy curves as functions of the MUT in Fig. 15(a) and by the bar chart comparing passive and adaptive total energy in Fig. 15(b).

Note that for both cases (cantilever and simply supported), if the characteristic loads are set lower than the 85th percentile, there is no further significant loss in the energy savings. This is because although higher levels of the load are more likely to occur, the load distribution covers a smaller part of the service life and thus the operational energy

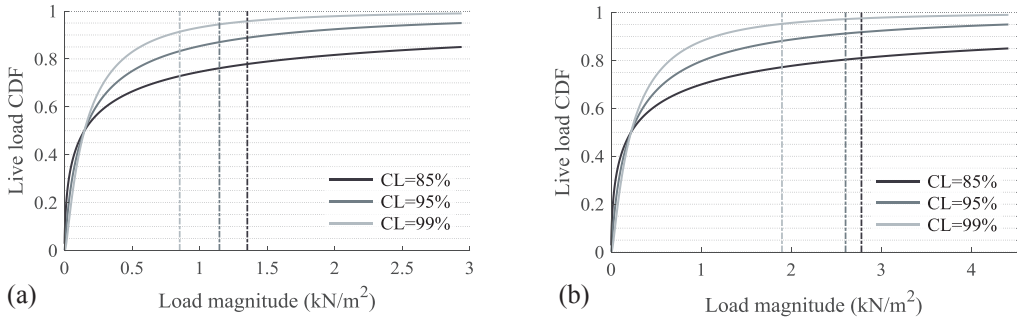

Fig. 13. Live load cumulative distribution functions (CDF) and activation thresholds. (a) cantilever, (b) simply supported.

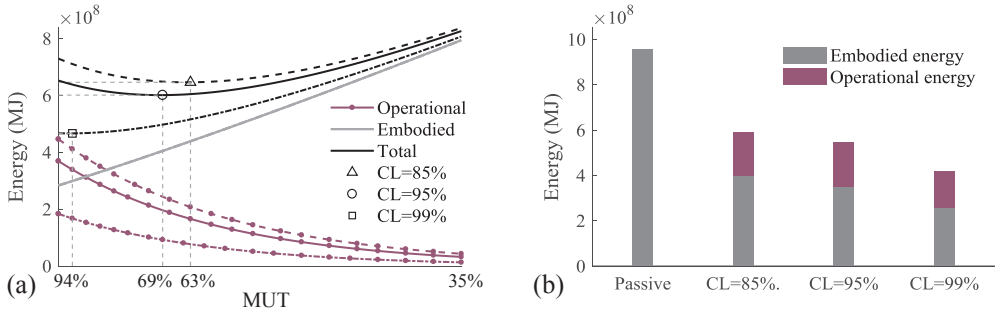

Fig. 14. Cantilever case; (a) total energy vs material utilisation factor (MUT) dashed CL = 85%, solid CL = 95%, dash-dot CL = 99% (CL = characteristic load); (b) comparison total energy.

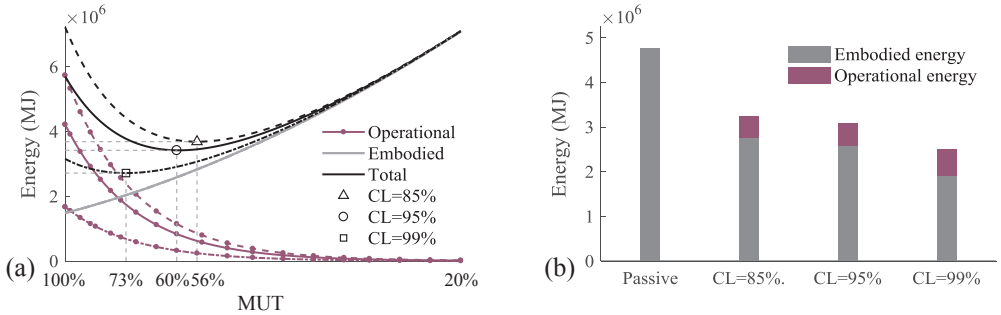

Fig. 15. Simply supported case; (a) total energy vs material utilisation factor (MUT) dashed CL = 85%; solid CL = 95%; dash-dot CL = 99% (CL = characteristic load); (b) comparison total energy.

consumption does not increase. Therefore, the energy savings sensitivity to the probability of occurrence of the live load is low. Given a certain load probability distribution, the characteristics loads do not represent a critical consideration for adaptive designs.

6. Energy savings vs live-to-dead-load and geometry

6.1. Settings

In this section the performances of the same statically determinate structural configurations described in 3.4 are studied in relation to the live-to-dead-load (L/D) ratio as well as the height-to-depth (H/D) for the cantilever or the span-to-depth (S/D) ratio for the simply supported case. For both cases, the L/D ratio will be varied in a 0.1 to 2 range to benchmark performances from low level loads to strong hazard events.

For the cantilever case, the height will be varied from 50 m to 800 m and the H/D ratio will be varied in a 2–20 range going from deep to very slender high-rise structures. The span of the simply supported truss will be varied from 20 m to 200 m and the S/D ratio will be varied in a 4–40 range going from deep to shallow roof truss systems.

6.2. Cantilever case | live-to-dead-load (L/D) ratio vs height

An optimum configuration minimising the total energy is obtained for each height sample in the range 50–800 m with a step of 50 m and the L/D ratio in the range 0.1–2 with a step of 0.1. The H/D ratio is kept

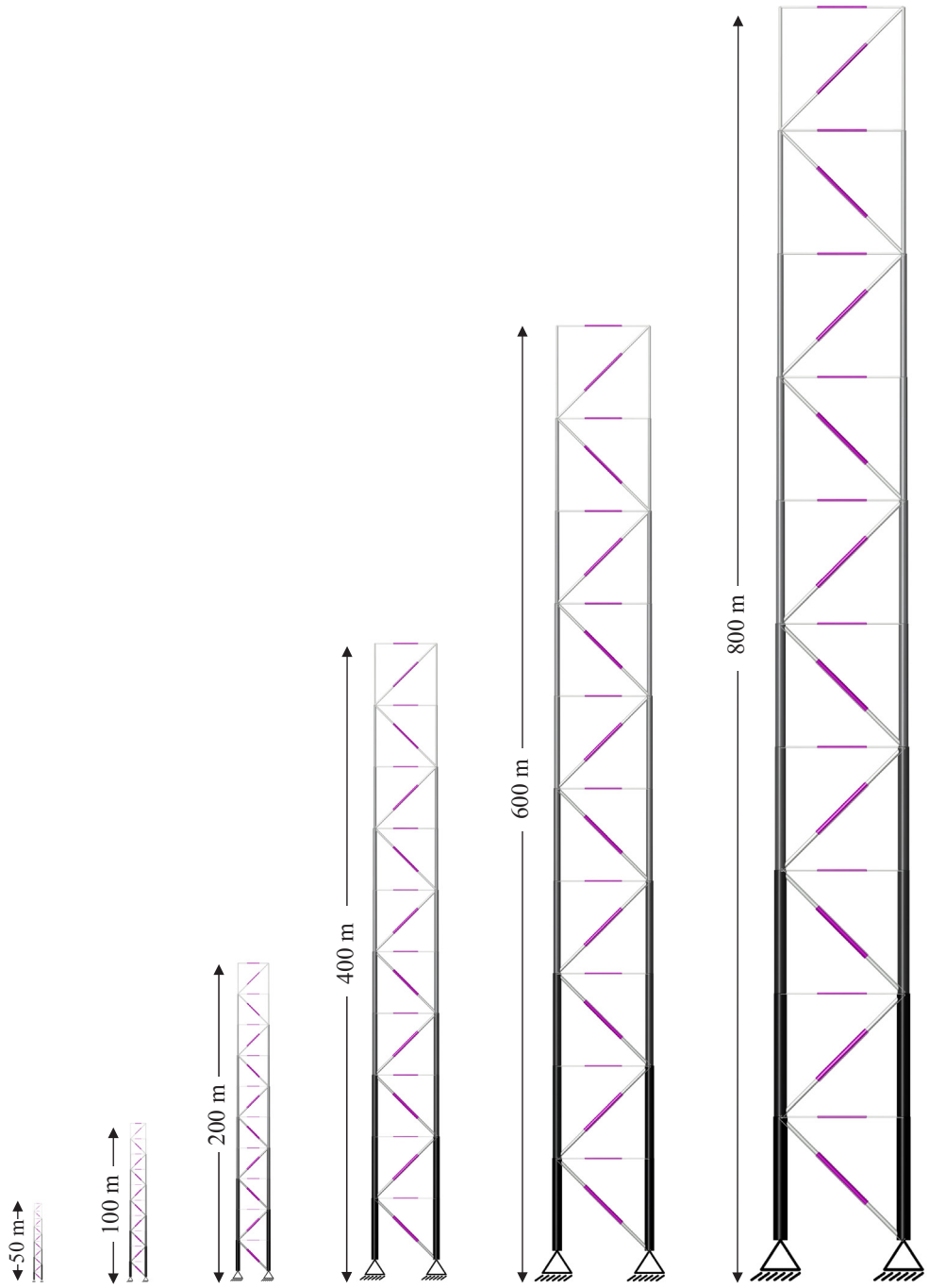

Fig. 16. Cantilever trusses 50 m to 800 m height, live-to-dead-load ratio L/D = 1. Scale 1:3000.

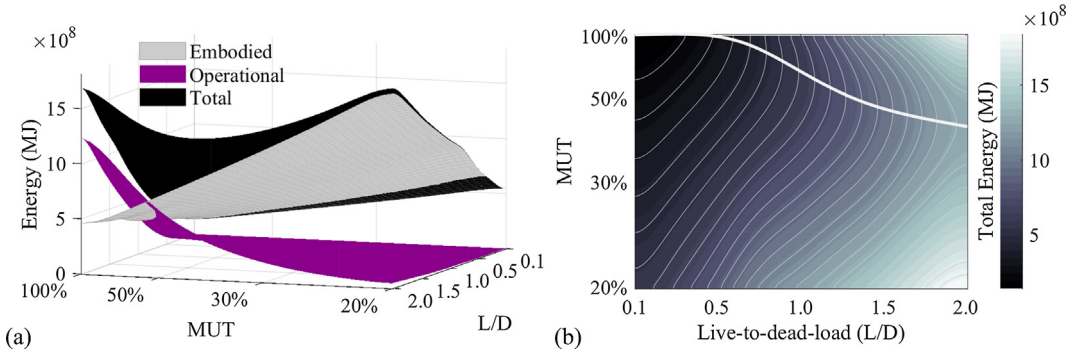

Fig. 17. (a) Embodied, Operational and Total energy vs live-to-dead-load (L/D) ratio and material utilisation factor (MUT); (b) Total vs L/D ratio and MUT. Height = 400 m.

constant at 10 because it is mid value in the range (2–20) that will be analysed in Section 6.4. The H/D ratio applies to both the in-plane and out-of-plane depths of the structure (refer to Fig. 4). To illustrate some of the configurations discussed in this section, Fig. 16 shows the optimised adaptive solutions drawn to scale at six different heights for a L/D ratio of 1.

Fig. 17(a) shows a surface plot of the whole-life energy as a function of the MUT and the L/D ratio for the 400 m height sample. This plot is a three-dimensional extension of the two-dimensional embodied-operational energy vs MUT graph shown previously. For clarity, the total energy is shown again in Fig. 17(b) as a contour map where the thick curve is the locus of the optimal MUT (minimum energy) for each L/D ratio. The MUT decreases as the L/D ratio increases because deflections must be limited using an optimal combination of structural mass and active control. The contribution of the structural mass to limit deflections is efficient at high L/D ratios and therefore the minimum energy design is obtained for lower levels of the MUT as the L/D ratio increases.

Fig. 18 (a) and (b) shows a surface plot and a contour map of the total energy as a function of the MUT and the height for a L/D ratio of 1. The MUT increases substantially as the height increases going from a minimum of 20% for the 50 m sample up to 100% for the 800 m sample. Referring to Fig. 18(a), it can be seen that for tall structures, as the MUT decreases, the embodied energy increases at much faster rate than the decrease in operational energy hence shifting the optimum towards higher MUTs. Conversely, for low height structures it is more effective to use structural mass to limit deflections rather than operational energy.

Therefore, to minimise the whole-life energy, the load activation threshold must be pushed to high values for low height structures as indicated in Fig. 19 which shows the live load CDF and the activation thresholds represented as dashed-dot lines. In other words, the taller the structure the better utilised is the material.

From the observation that operational energy becomes dominant over embodied energy at high L/D ratios and material is better utilised in tall structures, it follows the energy saving behaviour as a function of the L/D ratio shown in Fig. 20(a) for each height sample. The mass

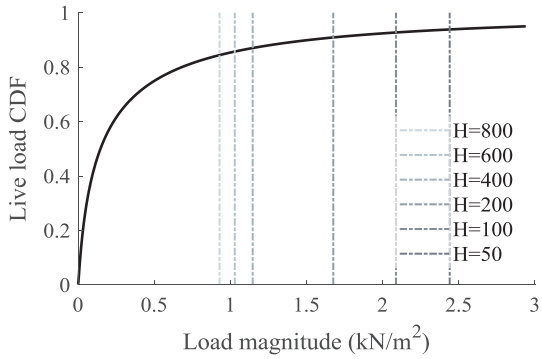

Fig. 19. Live load cumulative distribution function (CDF) and activation thresholds at live-to-dead-load ratio L/D = 1.

saving curves are very similar and therefore are not shown here. Both energy and mass savings increase substantially with the height up to 45% and 65% respectively. Because all energy saving curves have a maximum, it means that as the live load increases it is effective to use actuation for deflection control until the operational energy becomes dominant over the embodied energy after which passive stiffness (i.e. structural mass) must be used to lower the whole-life energy.

The energy savings reach maxima indicated by dots in Fig. 20(a) for a higher L/D ratio as the height increases. This means that low height structures perform better than taller ones at a low L/D ratio thus matching real-world scenarios in which the probability of occurrence of a high intensity live load (i.e. wind) is higher for tall buildings.

The total time of actuation as a function of the L/D ratio has a very similar behaviour to that of the energy savings. The actuation time maxima also increase as the height increases going from approximately 1 year for the 50 m height sample at a L/D ratio of 0.1 to 6 years for the 800 m height sample at a L/D ratio of 2. Fig. 20(b) shows the maximum actuator length change as a function of the L/D ratio for each height sample. Although the operational energy is the highest at large spans and high L/D ratios, the actuator length changes remain small (less than

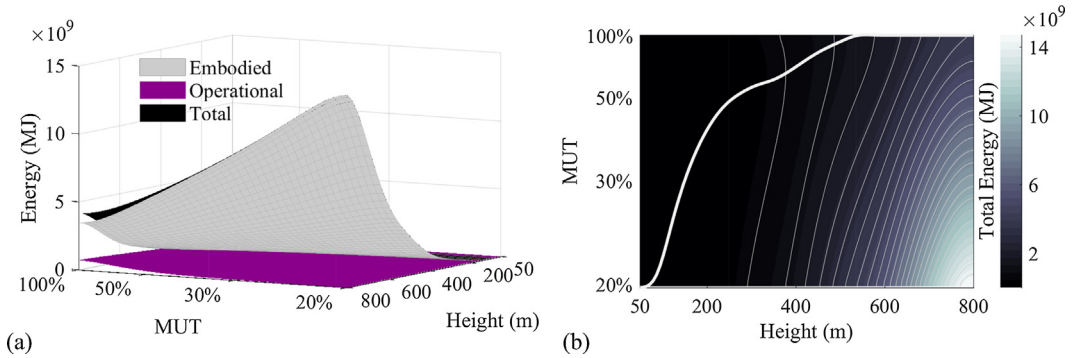

Fig. 18. (a) Embodied, Operational and Total energy vs Height and material utilisation factor (MUT); (b) Total energy vs Height and MUT. Height = 400 m.

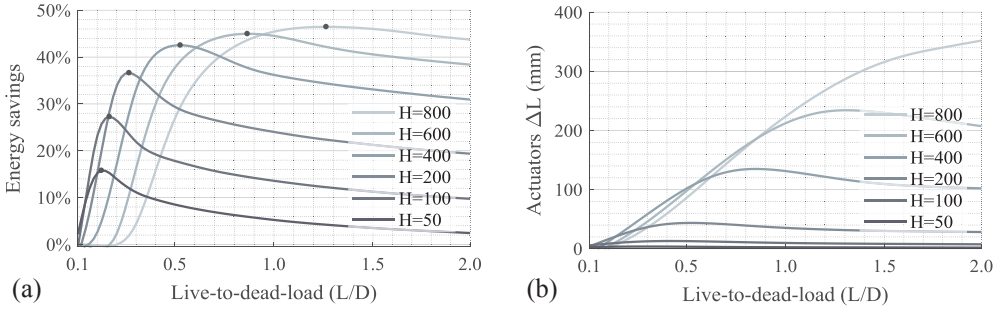

Fig. 20. (a) Energy savings and (b) actuator max length change vs live-to-dead-load ratio (L/D).

400 mm). Minimum actuator control effort is obtained as a result of the optimal actuator placement method formulated in Senatore et al. [37].

6.3. Simply supported case | live-to-dead-load (L/D) ratio vs span

An optimum configuration minimising the total energy is obtained for each span and L/D ratio. The S/D ratio is kept constant at 20 because it is mid-value in the range that will be analysed in Section 6.5. To illustrate some of the configurations discussed in this section, Fig. 21 shows the optimised adaptive solutions drawn to scale at six different spans for a L/D ratio of 1.

The whole-life energy as a function of the MUT and L/D ratio is similar to the cantilever case (see Fig. 17a). Given a certain span, the contribution of the structural mass to limit deflections is efficient at high L/D ratios because the operational energy becomes dominant over the embodied energy and therefore the minimum energy design is obtained for lower levels of the MUT as the L/D ratio increases.

Fig. 22(a) and (b) show the contour map of the total energy as a function of the MUT and the span at a L/D ratio of 0.5 and 1.5 respectively. In the first case (Fig. 22a), the MUT remains fixed at 100% (indicated by a dash-dot line). However, when the L/D ratio is larger than 1.0 (Fig. 22b) the MUT increases as the span increases. To explain this behaviour, it is useful to refer to Figs. 23 and 24 which show the controlled shape (a), non-controlled (or deformed) shape (b) and load-path (c) for a 100-m span simply supported truss under LC2 at L/D ratios of 0.5 and 1.5 respectively. As explained in Section 3.3, the adaptive structure takes the live load already stressed due to the displacement compensation under permanent load. In this case the structure is kept perfectly flat under the permanent load. The diagonal members hosting the actuators are in compression having made positive length changes (expansion) to compensate for the downward permanent load. When the live load is lower than the dead load little displacement compensation is needed (Fig. 23b and c). The actuators are required to make a length reduction under compressive forces (negative work) and thus very little or null operational energy is needed. For this reason, the MUT can stay fixed at 100% because in this

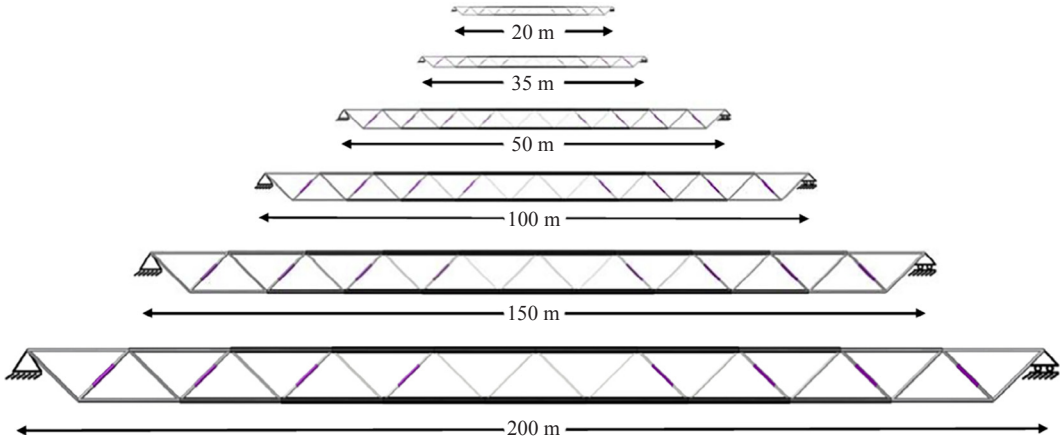

Fig. 21. Simply supported trusses 20 m to 200 m span, live-to-dead-load ratio L/D = 1. Scale 1:1500.

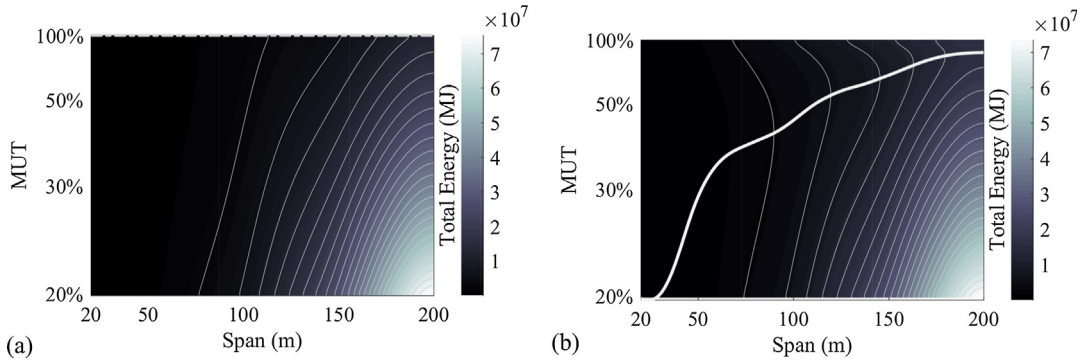

Fig. 22. Total energy vs material utilisation factor (MUT) and Span, live-to-dead-load ratios (a) L/D = 0.5 (b) L/D = 1.5.

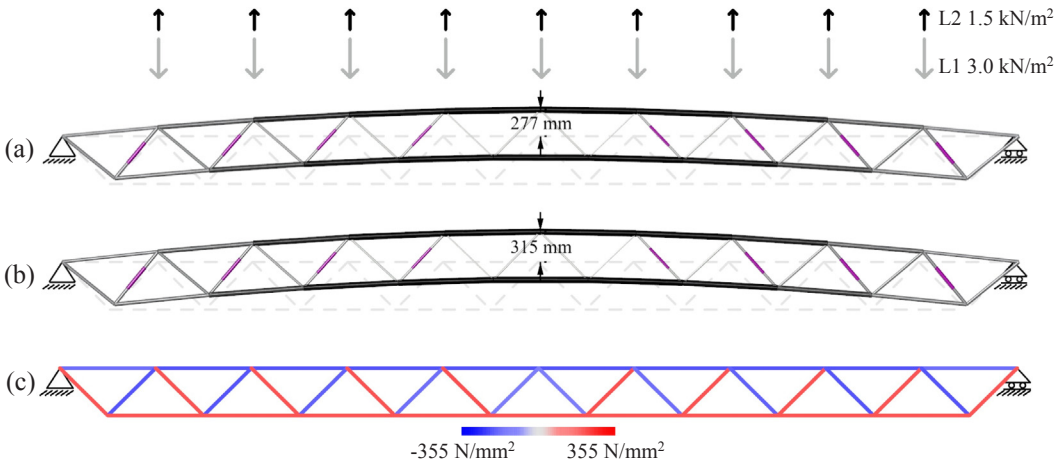

Fig. 23. 100-m span simply supported truss (a) controlled shape, (b) non-controlled shape and (c) optimal load-path under LC2; live-to-dead-load ratio L/D = 0.5. Mag. ×10, scale 1:800.

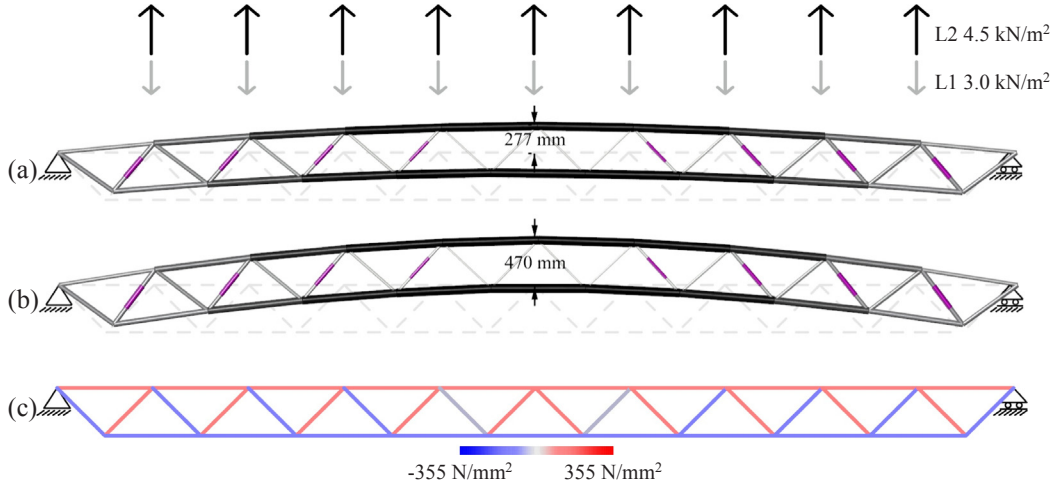

Fig. 24. 100-m span simply supported truss (a) controlled shape, (b) non-controlled shape and (c) optimal load-path under LC2; live-to-dead-load ratio L/D = 1.5. Mag. ×10, scale 1:800.

case it is more efficient to use little operational energy than to add structural mass regardless of the span of the structure. When the live load is larger than the dead load, displacement compensation becomes substantial and the stresses in the diagonal members hosting the actuators reverse from compression to tension (Fig. 24b and c). Since the actuators are required to reduce their length whilst being in tension (positive work), the operational energy increases substantially. For this reason, for L/D ratios larger than 1, the MUT increases as the span increases going from a minimum of 20% to 100% for large spans (> 150 m) as shown in Fig. 22(b).

The change in behaviour that occurs when the L/D ratio becomes larger than unity can also be seen by analysing the activation threshold. Fig. 25(a) and (b) show the activation thresholds (dashed-dot lines) on the plot of the live load cumulative distribution functions for a L/D ratio of 0.5 and 1.5 respectively. In the first case the activation thresholds are similar regardless of the span because the MUT remains fixed at 100%. By contrast, when the L/D ratio is 1.5, as expected the activation threshold is higher for small span structures because it takes higher loads to reach the deflection limits.

Fig. 26(a) plots the energy savings as a function of the L/D ratio for

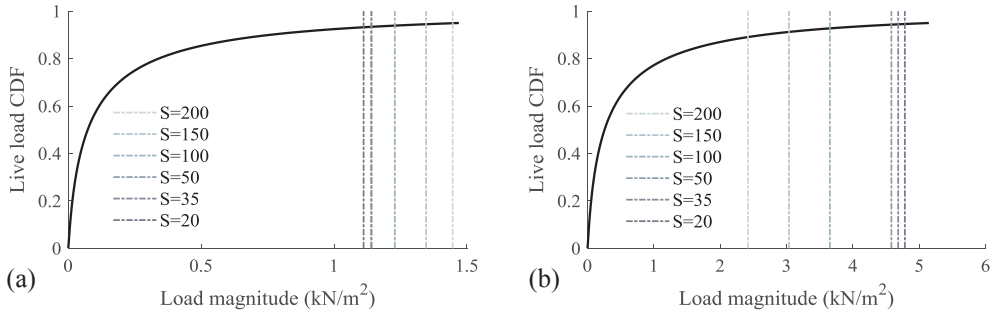

Fig. 25. Activation thresholds at (a) live-to-dead-load ratio L/D = 0.5 and (b) live-to-dead-load ratio L/D = 1.5.

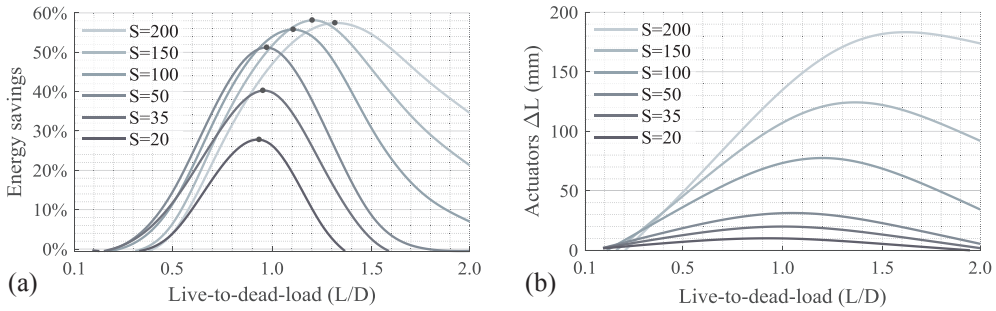

Fig. 26. (a) Energy savings and (b) actuator max length change vs live-to-dead-load ratio (L/D).

each span. As observed for the cantilever case, the energy savings increase for all spans as the L/D ratio increases. The savings reach maxima (indicated by dots) in Fig. 26(a) at higher L/D ratios as the span increases. After reaching maxima, the energy savings decrease more rapidly than what was observed for the cantilever case. This is caused by different boundary conditions and the way the live load relates to the dead load for the two cases. As explained in Section 3.4, the L/D ratio is the ratio between the live load and dead load without considering their application area. For the simply supported case (which is thought of as a roof support system), both live load and dead load application areas are identical. For the cantilever case instead (which is thought of as a multi-storey building) the dead load application area is the sum of all floor areas and the live load one is the façade area. For this reason, as the height of the cantilever structure increases, the dead load becomes dominant over the live load. This means that for the same L/D ratio, the live load resultant is comparatively higher with respect to the dead load resultant at low heights. This explains why for the cantilever case the operational energy increases at a lower rate as the L/D ratio increases and thus the energy savings decrease more gradually with respect to the simply supported case.

As for the cantilever case, the total time of actuation as a function of the L/D ratio has very similar behaviour to that of the energy savings. The actuation time maxima increase as the span increases going from approximately 3 years for the 20 m span sample at a L/D ratio of 1 to 4.4 years for the 200 m height sample at a L/D ratio of 1.5. Fig. 26(b) shows that the actuator length changes remain small (less than 250 mm) even for long spans and high L/D ratios.

6.4. Cantilever case|height-to-depth ratio vs height

This section presents a study concerning the influence of the height-to-depth (H/D) ratio (i.e. slenderness) on the energy savings for the cantilever case. When studying the influence of the L/D ratio on the energy savings, the H/D ratio was kept constant at 10. In this study the

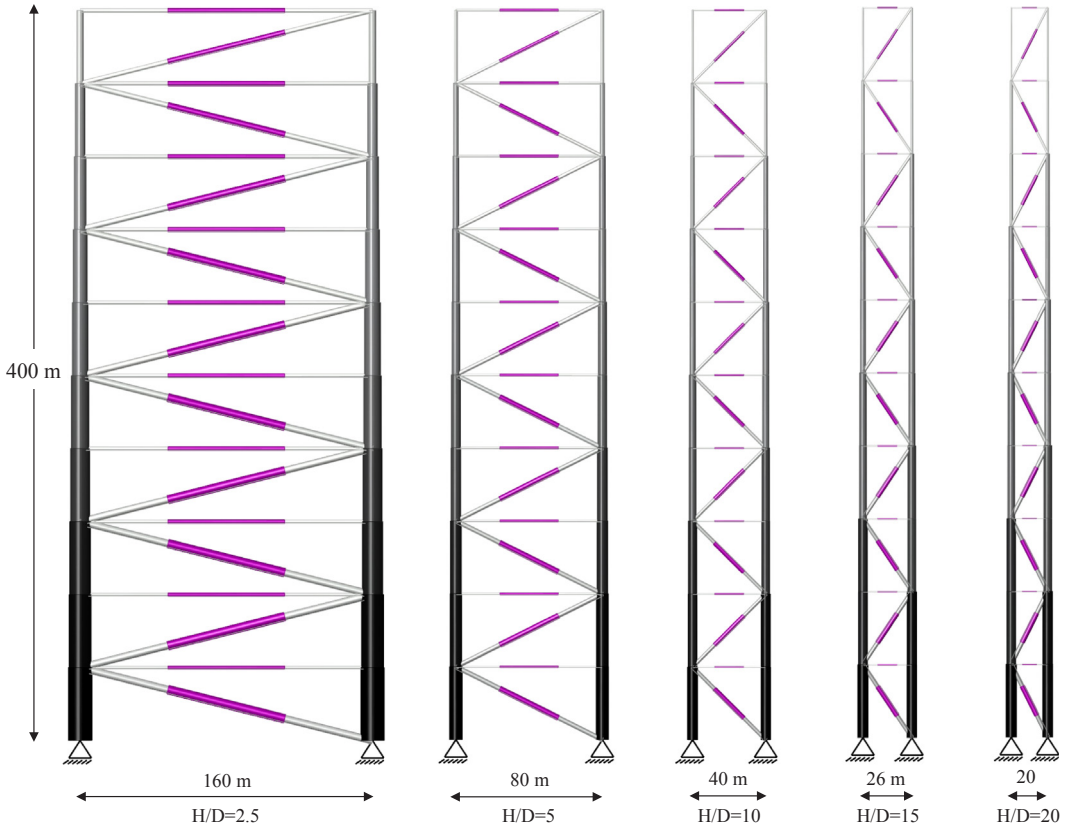

Fig. 27. 400-m height cantilever trusses, L/D = 1, height-to-depth ratio H/D from 2.5 to 20. Scale 1:4000.

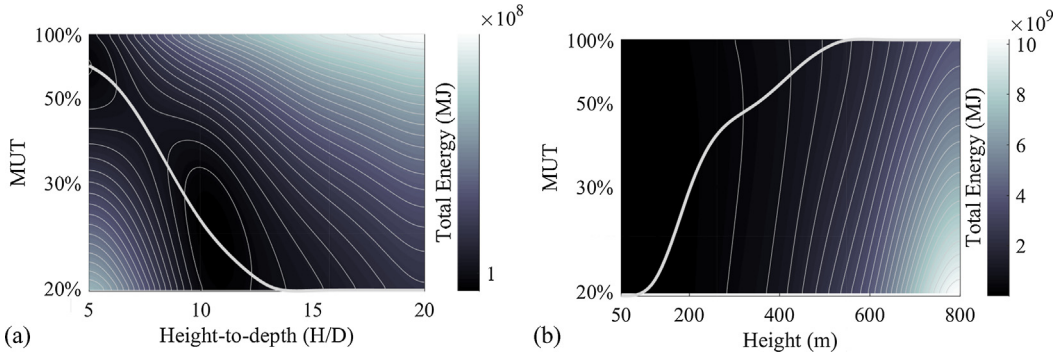

Fig. 28. (a) Total energy vs Height-to-depth (H/D) ratio and material utilisation factor (MUT), height = 400 m; (b) Total energy vs Height and MUT, H/D = 10.

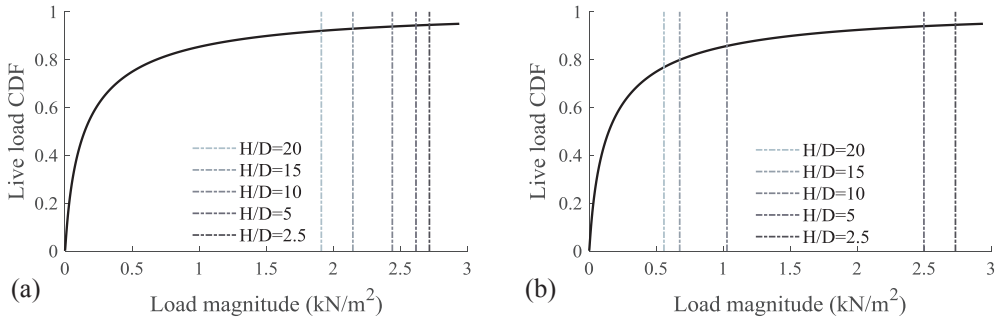

Fig. 29. Live load cumulative distribution and activation thresholds (a) height = 50 m, (b) height = 400 m.

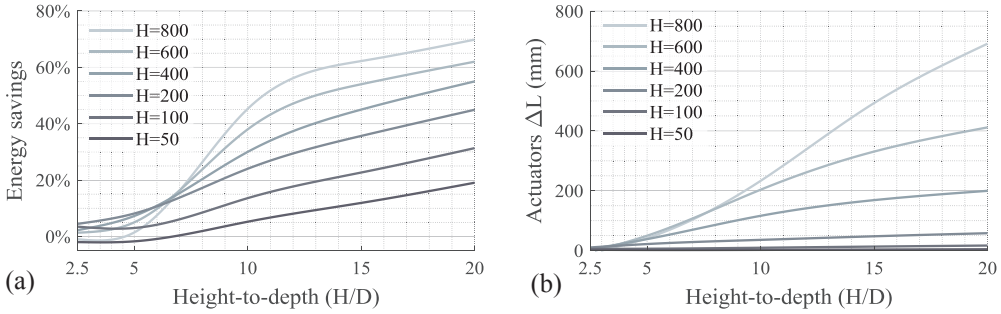

Fig. 30. (a) Energy savings and (b) actuator max length change vs height-to-depth ratio (H/D).

H/D ratio will be varied between 5 and 20 going from deep to very slender structures. The L/D ratio will be kept at 1 because it is mid-value of the range that has been explored in Section 6.2. An optimum configuration that minimises the total energy is obtained for each H/D ratio and height. Fig. 27 shows the optimised adaptive solutions drawn to scale for a height of 400 m.

Fig. 28(a) shows a contour map of the total energy as a function of the MUT and H/D ratio. The thick curve is the locus of optimal MUTs. Increasing the H/D ratio favours adaptive structures because the actuators can control deflections no matter how slender the structure is. However, at high H/D ratios the operational energy is high because deflection limits are reached for lower levels of the live load. For this reason, the contribution of the structural mass to limit deflections is effective at high H/D ratios and therefore the minimum energy design is obtained for lower levels of the MUT.

Fig. 28(b) shows a contour map of the total energy as a function of the MUT and the height for a H/D ratio of 10. The MUT increases substantially as the height increases going from a minimum of 20% for low heights (50 m) to 100% for tall structures (500–800 m). This is because for tall structures the operational energy decreases at a slower rate than the increase in embodied energy hence shifting the optimum towards higher MUTs. In other words, for tall structures it is effective to control deflection using active control resulting in a very efficient material utilisation.

Fig. 29(a) and (b) show the plot of the live load CDF and the activation thresholds represented by dash-dot lines for the 50 m and 800 m height samples respectively. In both cases, the load activation threshold decreases as the structure becomes more slender. As the H/D ratio increases, deflection limits are reached for lower levels of the live load. The load activation threshold varies substantially for the 800 m height sample going from almost the design load value for deep structures (H/D = 2.5 and H/D = 5) to a very low value for more slender structures. This is because for tall and deep structures, the dead load resultant is much larger than the live load resultant and thus little displacement compensation is needed. When the H/D ratio increases, the live load resultant increases substantially up to 40% the value of the dead load resultant and therefore the load activation threshold also decreases substantially.

Fig. 30(a) shows the plot of the energy savings as a function of the H/D ratio for each height sample. As expected the energy savings increase as the H/D ratio increases for all height samples. The large difference in the load activation threshold between deep and slender tall

structures (Fig. 29b) explains the drastic increase in the energy savings for the height samples above 400 m. There are no substantial savings for deep and low height structures (S/D of 2.5 and H = 50). However, for H/D ratios larger than 5, the savings become substantial at all heights reaching 70% for the 800 m height sample.

The actuation time is substantial at all heights from a H/D ratio larger than 5 reaching almost a quarter of the service life (50 years) for tall structures. For deep (H/D = 5) and low height structures no actuation is needed. Fig. 30(b) shows the plot of the maximum actuator length changes as a function of the H/D ratio for each height sample. The maximum length change does not exceed 700 mm even for the 800 m span sample.

6.5. Simply supported case | span-to-depth ratio vs span

This section presents a study concerning the influence of the span-to-depth (S/D) ratio (i.e. slenderness) on the energy savings for the simply supported truss case. The S/D ratio will be varied from 5 to 40 going from deep to very slender structures. The L/D ratio is set to 1 because it is mid value of the range that was analysed in Section 6.3. To illustrate some of the configurations discussed in this section Fig. 31 shows the 100-m span adaptive solutions for five S/D ratios.

Fig. 32 shows the contour map of the total energy as: (a) a function of the MUT and S/D ratio for the 100-m span sample; (b) a function of the MUT and span for a S/D ratio of 20. Both contour maps show that the minimum energy design is obtained for a MUT of 100% at all S/D ratios and spans. This is because the L/D ratio is kept at 1 and the live load is identical but opposite in direction to the dead load. For this reason, little displacement compensation is needed and thus the material can be fully utilised without causing any substantial increase in operational energy to reduce deflection actively.

Fig. 33 shows the plot of the live load CDF and the load activation thresholds represented by dash-dot lines for (a) the 100-m span sample at all S/D ratios and (b) for an S/D ratio of 40 at all spans. The load activation threshold decreases as the S/D ratio increases because the structure becomes more slender and therefore it takes lower levels of the live load to reach deflection limits. However, the activation threshold increases with the span because the minimum energy design is obtained for an MUT of 100% regardless of the span. This is because as the span increases the cross section area lower bound must be increased to obtain feasible solutions resulting in a higher value of the load activation threshold.

Fig. 34(a) shows the plot of the energy savings as a function of the S/D ratio for each span sample. Although the energy savings are negligible for deep structures (S/D of 5), they increase rapidly above 20% for all spans as the S/D ratio increases to 10. The savings continue to increase steadily reaching 50% for an S/D ratio of 20 and up to 70% for an S/D ratio of 40. In this case, the span has little influence on the energy savings because for L/D ratios smaller or equal to unity, the minimum energy design is obtained for an MUT of 100% regardless the

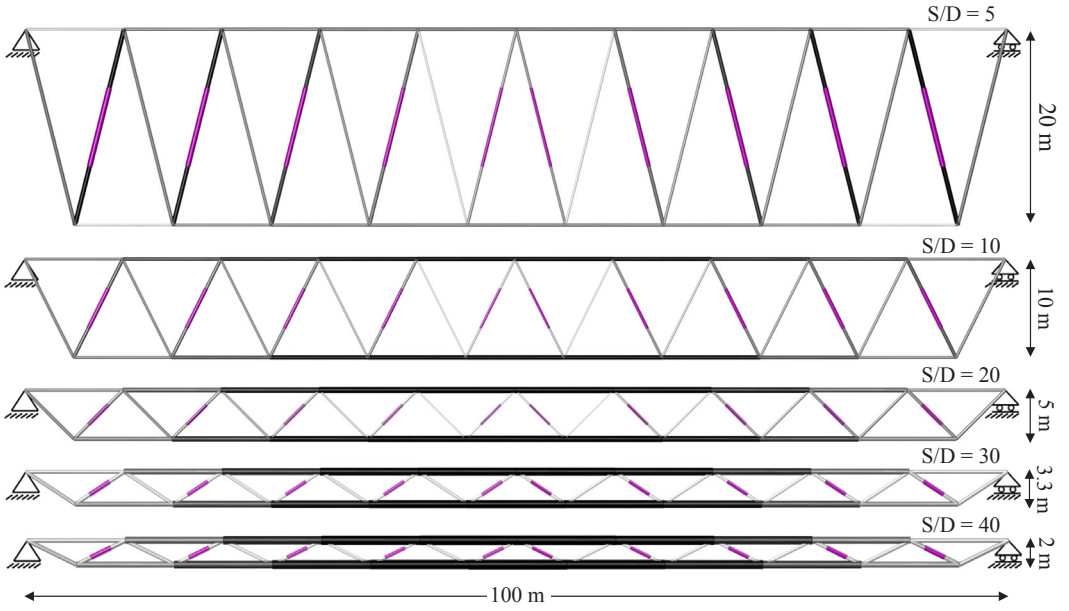

Fig. 31. 100-m span simply supported trusses, L/D = 1, span-to-depth ratio S/D from 5 to 40. Scale 1:800.

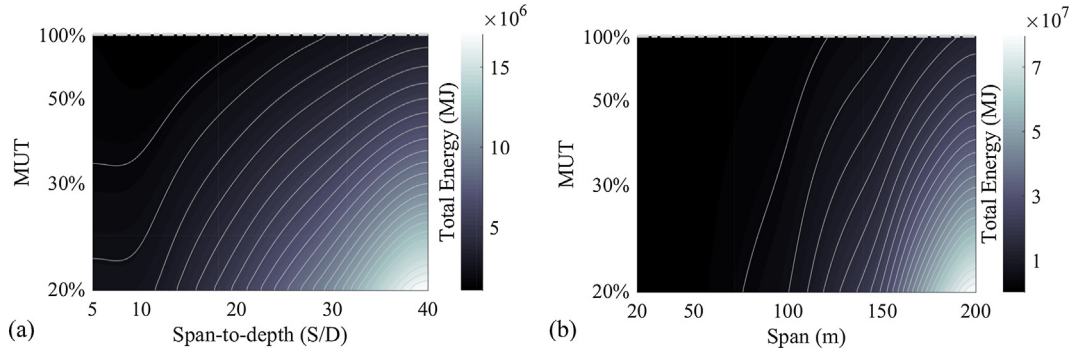

Fig. 32. Total vs Span-to-depth ratio and material utilisation factor (MUT), span = 100 m; (b) Total vs Span and MUT, span-to-depth ratio S/D = 10.

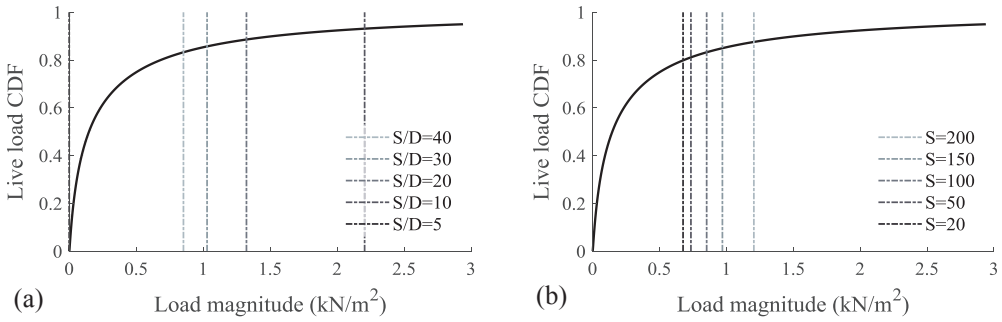

Fig. 33. Live load cumulative distribution function CDF and activation thresholds, (a) span = 100 m and (b) span-to-depth ratio S/D = 40.

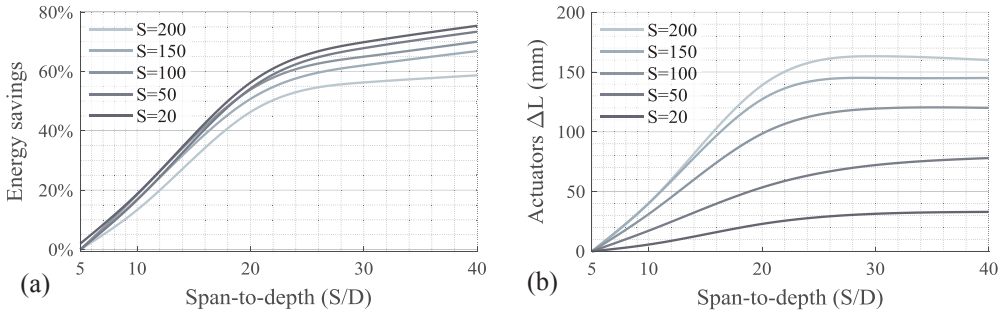

Fig. 34. (a) Energy savings and (b) operational energy vs span-to-depth ratio (S/D).

S/D ratio and the span.

The actuation time is substantial at all spans from a S/D ratio larger than 10 reaching a fifth of the service life (50 years) for slender structures. For deep structures (S/D = 5) no actuation is needed. The maximum actuator length change does not exceed 200 mm even for the 200 m span at a S/D ratio of 40 as shown in Fig. 34(b).

7. Monetary cost analysis

7.1. Introduction

A monetary cost analysis is carried out for the same set of structures considered in Section 6. The aim is to appreciate how the adaptive solution compares to the passive one in monetary cost terms. Input parameters are identical to the previous study on energy savings. Monetary costs are evaluated in relation to the live-to-dead-load (L/D) ratio, the height-to-depth H/D or span-to-depth (S/D) ratio as well as the height or span for the cantilever and simply supported case respectively. To run the monetary cost analysis some assumptions have been made:

- Actuation is hydraulic. The cost of a hydraulic actuator is assumed to be linearly proportional to the required force [45] at a rate of 0.97 £/kN (e.g. an actuator with a push/pull force of 1000 ton costs £ 9700). The cost of the hydraulic system (e.g. pumps, loading manifold assembly) and driver electronics is estimated at £5000/actuator [45].
- Element stresses are monitored using strain gauges. The average cost per strain gauge sensor (full-bridge type) is set to £500/unit including lead wires and signal amplification [46].
- The cost for data acquisition (i.e. monitoring) and processing is set to £500 per channel – one channel per strain sensor, two channels (position feedback and power output) per actuator.
- The cost of construction material (in this case steel) is set to £3000/tonnage [47]. This figure mostly depends on the building type usually varying between £1000 and £5000 per tonnage depending on specifications (e.g. office vs landmark building).
- The cost of fabrication for the passive and the adaptive structure is assumed to be identical because both structures require fabrication of an equal number of joints and elements. Because the passive structure is generally substantially heavier than the adaptive one, it is likely that fabrication costs will be higher for the former due to logistics.
- Control system maintenance costs include inspections as well as replacements. It is assumed that an inspection is scheduled once per year taking one engineer a full-day to examine 5 actuators and 10 sensors. The cost of one inspection is set to £500 per day. In addition, it is assumed that up to 20% of the actuators and sensors will have to be replaced once during service life and thus an additional cost for replacement is accounted for.

7.2. Monetary cost analysis

Fig. 35(a) shows the plot of the monetary cost difference (adaptive minus passive) as a function of the height and the L/D ratio for the cantilever case. For L/D ratios larger than 0.5, the adaptive solution competes and eventually becomes less expensive as the height of the structure and the L/D ratio increases. For tall structures, the large difference in mass between the passive and the adaptive solution results in a monetary gain that outweighs the extra expenditure for sensors, actuators and control system. The adaptive structure becomes less expensive the higher the L/D ratio because it is increasingly more difficult for the passive structure to meet deflection limits by adding more material.

This monetary cost trend is also caused by the variation of the actuator and sensor density that is the number of actuators and sensors per cubic meter of structure (the volume occupied by the material used by the structure). Fig. 35(b) shows the plot of the actuator density as a function of the height and the L/D ratio. The actuator density decreases rapidly as the height and the L/D ratio increases because the structural topology remains fixed while the mass increases substantially. The sensor density as a function of the height and L/D ratio has a similar behaviour. Therefore, the control system cost share becomes less important as the height and the L/D ratio increases. The same applies when varying the height-to-depth (H/D) ratio, the higher the H/D ratio the more the adaptive structure becomes competitive in terms of

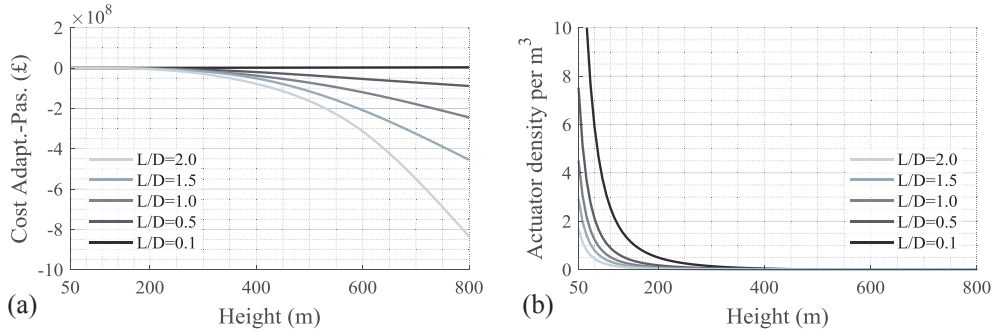

Fig. 35. Monetary cost (adaptive-passive); (a) cantilever; (b) simply supported.

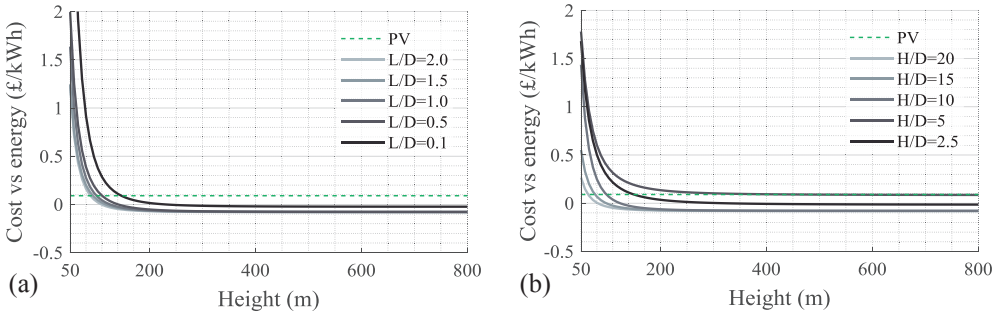

Fig. 36. Cost (£) of energy savings vs cost (£) of photovoltaics (PV); (a) cantilever; (b) simply supported.

monetary costs. Above an H/D ratio of 5, the adaptive cantilever truss is less expensive than the passive one at all heights. Similar results are obtained for the simply supported case. For L/D ratios larger than 1, span-to-depth (S/D) ratios larger than 20 and spans longer than 100 m, the adaptive solution is less expensive than the passive one.

If adaptive structures are intended as energy saving devices, the monetary cost of saving energy using structural adaptation can be compared to the cost of producing energy using other technologies. For instance, the cost per kWh of energy saved using actuation can be benchmarked against the cost of producing energy using photovoltaic panels (PV). In fact, the adaptive minus passive monetary cost difference (Fig. 35a) divided by the energy difference between the two solutions represents the cost of saving energy using structural adaptation. Fig. 36(a) and (b) shows the plot of the cost of saving energy for the cantilever case as a function of the height at different L/D and H/D ratios respectively. The cost of saving energy using PVs (the dashed line) is taken from the National Renewable Energy Laboratory (NREL) using a performance calculator for grid-connected PV systems [48]. Setting the location to London gives an average cost of 0.09 £/KWh. The cost of saving energy via actuation is higher than that of producing energy via PVs for structures lower than 50 m regardless the L/D ratio. The two systems compare above a height of 50 m and L/D ratios above 0.5. Adaptive structures are more efficient than PVs for heights above 200 m regardless the L/D ratio. The same applies when varying the H/D ratio. For deep and short structures, the cost of saving energy via actuation is higher than that of producing energy using PVs. The two systems compare even for deep structures as the height increases. For heights above 200 m, adaptive structures are more efficient than PVs regardless the H/D ratio. Similar results are obtained for the simply supported case. The thresholds beyond which the cost of saving energy via structural adaptation is lower than that of producing energy using PVs are 100 m span, L/D ratio of 0.5 and S/D ratio of 20.

8. Application domain optimal region

To determine the boundaries of the region where adaptive structures outperform passive structures in terms of energy and monetary cost, the results shown in Section 6 and 7 are combined. Energy and monetary cost savings in percentage terms are averaged thus forming a unique value.

Regarding the cantilever case, Fig. 37(a) shows the contour map of the combined energy plus monetary cost savings as a function of height and L/D ratio for a H/D ratio of 10. The zero level set is indicated by a thick curve. The optimal region covers the majority of the domain excluding L/D ratios lower than 0.2 and heights lower than 150 m. Fig. 37(b) shows the combined energy plus monetary cost savings as a function of span and H/D ratio for a L/D ratio of 1. In this case the optimal region includes deep structures (H/D = 2) for heights above 200 m.

Regarding the simply supported case, Fig. 38 shows a contour map of the combined savings as a function of: (a) the span and L/D ratio for a S/D ratio of 20 and (b) the span and S/D ratio for a L/D ratio of 1. The optimal region in this case occupies the upper right hand corner. This is because the energy savings reach maxima for L/D ratios in a range from 0.5 and 1.5 (Fig. 26a) and the adaptive solution is generally more expensive than the passive one except for spans above 100 m and L/D ratios larger than 0.7 and S/D ratios larger than 20.

Although the optimal regions shown in Figs. 37 and 38 are different, similar conclusions can be drawn for the cantilever and a simply supported case study: it is most beneficial to use structural adaptation in energetic and monetary terms for tall or long span structures as well as for slender structures. This is broadly the type of structures that are stiffness governed.

The simulations described in previous sections were carried out using a material energy intensity factor (MEI) of 36.5 Ml/kg which is that for steel obtained from predominantly virgin materials (i.e. no recycled contents) [42]. The same set of structures has been analysed using an MEI of 15 MJ/kg which corresponds to secondary steel obtained from predominantly recycled contents. For both cantilever and simply supported case, although savings are reduced, the optimal regions preserve almost identical boundaries thus showing little sensitivity to the MEI.

Table 3 gives the degree of sensitivity of the energy and monetary cost savings in relation to the input parameters. The degree of

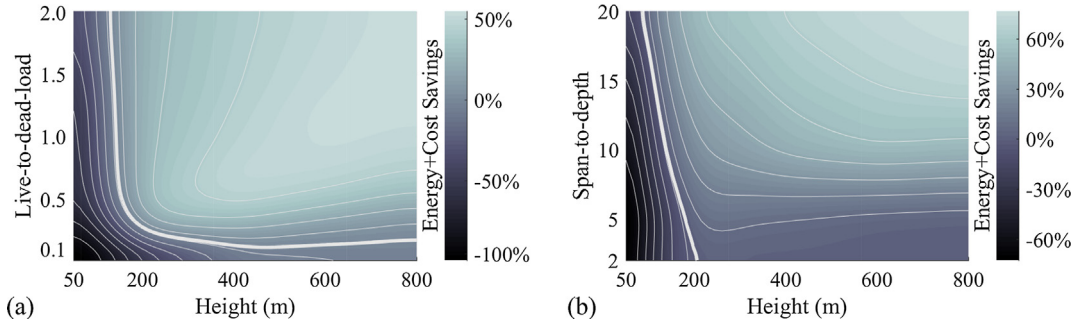

Fig. 37. Optimal region cantilever truss (a) height-to-depth ratio H/D = 10, (b) live-to-dead-load ratio L/D = 1. MEI = 36.5 MJ/kg; thick curves indicate zero level sets.

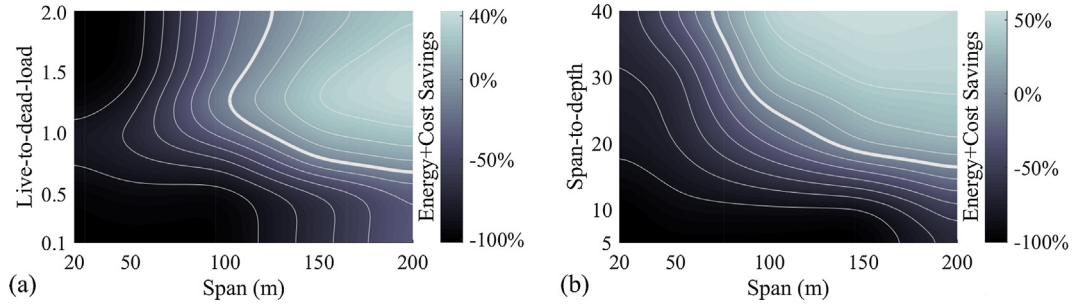

Fig. 38. Optimal region simply supported truss (a) span-to-depth ratio S/D = 20; (b) live-to-dead-load ratio L/D = 1. MEI = 36.5 MJ/kg, thick curves indicate zero level sets.

Table 3
Energy and monetary cost savings sensitivity.

Case	Live-to-dead-load	Span-to-depth	Characteristic load	MEI
Cantilever				
Height < 150 m	+ + +	+ + +	+	+
150 m < Height < 800 m	+	+	+	+
Simply supported				
Span < 100 m	+ + +	+ + +	+	+
100 m < Span < 200 m	+ +	+ +	+	+

Sensitivity: + little + + moderately + + + large.

sensitivity is a measure of how sensitive (i.e. small changes in the inputs generate big changes in the output) the performance metric is with respect to the input parameters.

The optimal region for the cantilever case is not very sensitive to either L/D or H/D ratios which is an important result because it shows that for this structural configuration there is a wide range of applicability including ordinary loading scenarios and deep structures.

Generally, it can be said that for high L/D ratios, low height or short span structures as well as for deep structures (i.e. low H/D or S/D ratios), it is not effective to use active control. When the L/D ratio is high the operational energy becomes dominant resulting in lower energy savings. In addition, for low height or small span structures as well as for deep structures, the monetary cost of the adaptive solution is generally higher than that of the passive one. Conversely for tall or long span structures as well as for slender structures (i.e. high H/D or S/D ratios), it is very effective to control deflections actively. In these cases, the adaptive solution is competitive in monetary terms with the passive solution and becomes cheaper as the height or span and the slenderness increase.

9. Conclusions

From the results of the parametric study presented in this paper it can be concluded that:

- Given a planar truss topology, the degree of static indeterminacy has little influence on the energy savings (Section 4);
- Given a certain load probability distribution, the characteristic loads do not represent a critical consideration for adaptive designs (Section 5);
- The energy savings as a function of the L/D ratio have a maximum. This is because for very strong live loads (high L/D ratios), the operational energy increases substantially resulting in lower energy savings. This is an important result because it shows that adaptive structures outperform passive ones not only for strong loading scenarios but also for ordinary cases (Section 6);
- Adaptive structures are more expensive than passive ones in terms of monetary costs for low heights or small spans as well as for deep structures. However, as either the height or the span or the slenderness increases or when stringent deflection limits are required, the adaptive solution becomes increasingly less expensive than the passive one (Section 7).
- Even in those cases when the adaptive design is more expensive, the extra cost with respect to a passive structure is not wasted but rather it is used to reduce the environmental impact of the structure. In this regard, adaptive structures can be thought of as energy saving devices. A comparison of the cost of saving energy using structural adaptation and that of producing energy using other technologies e.g. PV, shows that adaptive structures are efficient energy saving devices (Section 7).
- The optimal region in which adaptive structures outperform passive structures in energy and monetary cost terms is broadly the region of stiffness-governed structures (Section 8).

Adaptive structures also fulfil other functions such as being extremely slender and being capable of reducing deflections completely thus meeting strict deflection limits at the expense of a small amount of operational energy. This could bring several benefits including (1) buildings can be taller, roofs wider and bridges longer (2) buildings can have increased floor space via reduction of structural cores (3) people comfort and the overall structural integrity can be improved reducing deflections in real-time.

The structures taken into consideration in this article are reticular. Future work could look into whether these conclusions hold for frames as well as continuous structural types (e.g. slabs and shells).

Acknowledgements

The authors gratefully acknowledge the Engineering and Physical Sciences Research Council (EPSRC) who provided core funding for this project through UCL Doctoral Training Centre in Urban Sustainability and Resilience (Grant EP/G037698/1), as well as Expedition Engineering the project industrial partner who provided significant additional resources. EPFL Applied Computing and Mechanics Laboratory (IMAC) is thankfully acknowledged for their support during the review process of this article.

References

[1] Soong T, Chang J. Active vibration control of large flexible structures. Shock Vib Bull 1982;52:47–54.
[2] Soong TT. State of the art review: active structural control in civil engineering. Eng Struct 1988;10:74–84.
[3] Abdel-Rohman M, Leipholz H. Active control of tall buildings. J Struct Eng 1983;109(3):628–45.
[4] Reinhorn AST, Lin R, Riley M. Active bracing sytem: a full scale implementation of active control. Buffalo: National Center for Earthquake Engineering Research; 1992.
[5] Bani-Hani K, Ghaboussi J. Nonlinear structural control using neural networks. J Eng Mech 1998;124(3):319–27.
[6] Rodellar J, Mañosa V, Monroy C. An active tendon control scheme for cable-stayed bridges with model uncertainties and seismic excitation. Struct Control Health Monit 2002;9(1):75–94.
[7] Xu B, Wu S, Yokoyama K. Neural networks for decentralized control of cable-stayed bridge. J Bridge Eng (ASCE) 2003;8:229–36.
[8] Schnellenbach MH, Steiner D. Self-tuning closed-loop fuzzy logic control algorithm for adaptive prestressed structures. Struct Eng Int; 2013. p. 163–72.
[9] Preumont A, de Marneffe B, Deraemaeker A, Bossensb F. The damping of a truss structure with a piezoelectric transducer. Comput Struct 2008;86(3–5):227–39.
[10] Sobek W. Auf pneumatisch gestützten Schalungen hergestellte Betonschalen Doctoral dissertation Stuttgart: University of Stuttgart; 1987.
[11] Weilandt A. Adaptivität bei Flächentragwerken Doctoral dissertation Stuttgart: ILEK, University of Stuttgart; 2007.
[12] Neuhäuser S. Untersuchungen zur Homogenisierung von Spannungsfeldern bei adaptiven Schalentragwerken mittels Auflagerverschiebung Doctoral dissertation Stuttgart: ILEK, University of Stuttgart; 2014.
[13] Pellegrino S. Deployable structures. NewYork: SpringerWien; 2001.
[14] Henry A, Kam C, Smith M, Lewis C, King M, Boulter N, et al. Singapore sports hub: engineering the national stadium. The Structural Engineer, vol. 94, no. 9; 2016.
[15] Fuller B. Tensile-Integrity Structures. U.S. Patent 3,063,521; 1962.
[16] Calladine C. Buckminster Fuller's 'Tensegrity' structures and Clerk Maxwell's rules for the construction of stiff frames. Int J Solids Struct 1978;14:161–72.
[17] Skelton RE, de Oliveira MC. Tensegrity systems. New York: Springer; 2009.
[18] Tibert G. Deployable tensegrity structures for space applications Doctoral dissertation Stockholm: Royal Institute of Technology; 2002.
[19] Fest E, Shea K, Domer B, Smith F. Adjustable tensegrity structures. J Struct Eng 2003;129:515–26.
[20] Adam B, Smith IF. Active tensegrity: a control framework for an adaptive civil-engineering structure. Comput Struct 2008;86(23–24):2215–23.
[21] Veuve NSS, Smith I. Deployment of a tensegrity footbridge. J Struct Eng 2015;141(11):1–8.
[22] Santos FRA, Micheletti A. Design and experimental testing of an adaptive shape-morphing tensegrity structure, with frequency self-tuning capabilities, using shape-memory alloys. Smart Mater Struct 2015;24:1–10.
[23] Campanile LF. Initial thoughts on weight penalty effects in shape-adaptable systems. J Intell Mater Syst Struct 2005;16:47–56.
[24] Hasse A, Campanile LF. Design of compliant mechanisms with selective compliance. Smart Mater Struct 2009;18(11):115016.
[25] Jenkins C. Compliant structures in nature and engineering, 1st ed., WIT Press; 2005.
[26] Previtali F, Ermanni P. Performance of a non-tapered 3D morphing wing with integrated compliant ribs. J Smart Mater Struct 2012;21:1–12.
[27] Lienhard J, Schleicher S, Poppinga S, Masselter T, Milwich M, Speck T, et al. Flectofin: a hingeless flapping mechanism inspired by nature. Bioinspiration Biomimetics 2011;6:1–7.
[28] Soong T, Cimellaro G. Future directions in structural control. Struct Control Health Monit 2009;16:7–16.
[29] Korkmaz S. A review of active structural control: challenges for engineering informatics. Comput Struct 2011;89:2113–32.
[30] Teuffel P. Entwerfen adaptiver strukturen Doctoral dissertation Struttgart: University of Stuttgart - ILEK; 2004.
[31] Begg D, Liu X. On simultaneous optimization of smart structures - Part II: Algorithms and examples. Comput Methods Appl Mech Eng 2000;184:25–37.
[32] Sobek W, Teuffel P. Adaptive Systems in Architecture and Structural Engineering. In: Proc SPIE 4330, Smart Structures and Materials 2001: Smart Systems for Bridges, Structures, and Highways, Newport Beach, CA, United States; 2001.
[33] Utku S. Theory of Adaptive Structures: incorporating intelligence into engineered products. Boca Raban, Florida, U.S: CRC Press LLC; 1998.
[34] Senatore G, Duffour P, Hanna S, Labbe F, Winslow P. Adaptive structures for whole life energy savings. International Association for Shell and Spatial Structures (IASS), vol. 52, no. 4 December n. 170; 2011, p. 233–40. URL: < https://www.researchgate.net/publication/261724310_Adaptive_Structures_for_Whole_Life_Energy_Savings > .
[35] Senatore G, Duffour P, Winslow P. Whole-life energy and cost analysis of adaptive structures - case studies. J Struct Eng (ASCE); 2018 [in press]. http://dx.doi.org/10.1061/(ASCE)ST.1943-541X.0002075.
[36] Senatore G, Duffour P, Winslow P, Wise C. Shape control and whole-life energy assessment of an “Infinitely Stiff” prototype adaptive structure. Smart Mater Struct 2018;27(1):015022.
[37] Senatore G, Duffour P, Winslow P, Hanna S, Wise C. Designing adaptive structures for whole life energy savings. In: Proceedings of the fifth international conference on structural engineering, mechanics & computation, Cape Town, Taylor & Francis Group, London; 2013, p. 2105–10. URL: < https://www.researchgate.net/publication/261724301_Designing_adaptive_structures_for_whole_life_energy_savings > .
[38] Huber JE, Fleck NA, Ashby MF. The selection of mechanical actuators based on performance indices. Proceed Roy Soc A 1997;453(1965):2185–205.
[39] Senatore G. Adaptive building structures Doctoral Dissertation London: University College London; 2016.
[40] Patnaik S, Gendy A, Berke S, Hopkins D. Modified Fully Utilized Design (MFUD) method for stress and displacement constraints. Int J Numer Meth Eng 1998;41:1171–94.
[41] ENERPAC. “E328e Industrial Tools - Europe,” 2016. [Online]. Available: < http://www.enerpac.com/en-us/downloads > [accessed 12 07 2017].
[42] Hammond G, Jones C. Embodied energy and carbon in construction materials. Proceed Inst Civil Eng – Energy 2008;161(2):87–98.
[43] Griffis L. Serviceability limit states under wind load. Eng J 1993;30(1):1–16.
[44] Eurocode 1 Actions on structures, “Eurocode 1: Actions on structures — General actions — Part 1–4: Wind”; 1991.
[45] Colin T, Alister C. Interviewees, Quotation HQQ49103. [Interview]. 14 06; 2017.
[46] Vishay. [Online]. Available: < http://www.vishaypg.com/micro-measurements/ > ; 2015. [Accessed December 2015].
[47] TATA Steel. Sections Publications; 2012. [Online]. Available: < http://www.tatasteeleurope.com/en/products_and_services/products/long/sections/sections_publications/ > [accessed 18 March 2013].
[48] N.R.E.L. NREL, A Performance Calculator for Grid-Connected PV Systems, [Online]. Available: < http://rredc.nrel.gov/solar/calculators/PVWATTS/version1/ > ; 2012 [accessed 02 April 2012].